

THIRTEENTH QUARTERLY TECHNICAL PROGRESS REPORT

DOE CONTRACT NO. DE-AC22-86PC90013

Optimum Catalytic Process for Alcohol Fuels from Syngas

Pittsburgh Energy Technology Center

April 28, 1990

DISCLAIMER

This report was prepared as an account of work sponsored by an agency of the United States Government. Neither the United States Government nor any agency thereof, nor any of their employees, makes any warranty, express or implied, or assumes any legal liability or responsibility for the accuracy, completeness, or usefulness of any information, apparatus, product, or process disclosed, or represents that its use would not infringe privately owned rights. Reference herein to any specific commercial product, process, or service by trade name, trademark, manufacturer, or otherwise does not necessarily constitute or imply its endorsement, recommendation, or favoring by the United States Government or any agency thereof. The views and opinions of authors expressed herein do not necessarily state or reflect those of the United States Government or any agency thereof.

Solvents and Coatings Materials Division

Union Carbide Chemicals and Plastics Company Inc.

South Charleston Technical Center

South Charleston, West Virginia 25303

MASTER *de*

DISTRIBUTION OF THIS DOCUMENT IS UNLIMITED

**TECHNICAL PROGRESS REPORT
DE-AC22-86PC90013**

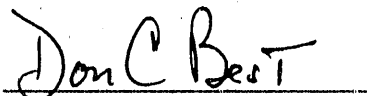
January - March, 1990

Optimum Catalytic Process for Alcohol Fuels from Syngas

Pittsburgh Energy Technology Center

Solvents and Coatings Materials Division

**Union Carbide Chemicals and Plastics Company Inc.
South Charleston Technical Center
South Charleston, West Virginia 25303**



**D. C. Best
Program Manager**

Patent Cleared by Chicago
OPC on May 22, 1990

Patent Hold

This document copy, since it is transmitted in advance of patent clearance, is made available in confidence solely for use in performance of work under contracts with the U.S. Department of Energy. This document is not to be published nor its contents otherwise disseminated or used for purposes other than specified above before patent approval for such release or use has been secured, upon request, from the Chief Office of Patent Counsel, U.S. Department of Energy, 9800 South Cass Avenue, Argonne, Illinois 60439.

DISCLAIMER

This Report was prepared as an account of work sponsored by the United States Government. Neither the United States nor the United States Department of Energy, nor any of their employees, makes any warranty, express or implied, or assumes any legal liability or responsibility for the accuracy, completeness, or usefulness of any information, apparatus, product, or process disclosed, or represents that its use would not infringe privately owned rights. Reference herein to any specific commercial product, process, or service by trade name, mark, manufacturer, or otherwise does not necessarily constitute or imply its endorsement, recommendation, or favoring by the United States Government or any agency thereof. The views and opinions of authors expressed herein do not necessarily state or reflect those of the United States Government or any agency thereof.

PATENT STATUS

This Technical Report is being transmitted in advance of DOE patent clearance and no further dissemination or publication shall be made of the Report without prior approval of the DOE Patent Counsel.

Patent Cleared by Chicago
OPC on May 22, 1990

CONTENTS

I. Contract Objectives	1
II. Schedule	2
III. Organization	3
IV. Summary of Progress	4
V. Changes	6
VI. Future Work	7

Appendixes

A. Use of Code System	9
B. Procedures for Catalyst Testing	10
C. Procedures for Product Analysis	11
D. Technical and Experimental Data	12

I. CONTRACT OBJECTIVES

The objectives of this contract are to discover and evaluate the catalytic properties of novel homogeneous, heterogeneous, or combination catalytic systems for the production of alcohol fuel extenders from syngas, to evaluate analytically and on the bench scale novel reactor concepts for use in converting syngas to liquid fuel products, and to develop on the bench scale the best combination of chemistry, reactor, and total process configuration to achieve the minimum product cost for conversion of syngas to liquid fuel products.

II. SCHEDULE

This program was planned as a 33-month research and development effort, extending through September, 1989.

The contract work is composed of three tasks. Task 1, the preparation of a Project Work Plan, has been completed. Task 2 comprises the chemical investigation of novel and existing catalysts for the production of fuel alcohols from syngas, either directly or through a step-wise process. Task 3 consists of engineering activities which will support the chemical investigations and develop economic evaluations and process conceptualization. Tasks 2 and 3 will proceed for the entire duration of the program.

In current work under Task 2, the effort has been mainly on heterogeneous catalysts. Novel systems which may exhibit superior behavior are being investigated.

Task 3 work has involved engineering support for the chemical investigations. Economic evaluations of a base case process for conversion of syngas to fuel alcohols were also pursued. Task 3 work has also involved experiments with selected catalytic systems. Current work in Task 3 includes the evaluation of slurry-catalyzed processes for the production of fuel alcohols or their derivatives.

A ten-month no-cost extension of this contract has been applied for and granted.

III. ORGANIZATION

The development of an optimum process for alcohol fuels from syngas is the goal of a research and development program conducted by a group within the Solvents and Coatings Materials Division of Union Carbide Corporation. During the initial portion of the contract, this group was part of the Engineering, Manufacturing and Technology Services Division.

The work is performed at Union Carbide Corporation's South Charleston Technical Center, South Charleston, West Virginia 25303.

Principal investigator is Dr. B. Duane Dombek.

Program manager is Dr. Donald C. Best.

IV. SUMMARY OF PROGRESS

A. Task 2: Catalyst Research

Work continues on optimization of higher alcohol catalysts consisting of transition metals supported on metal oxides with the spinel structure. Our work this quarter was designed to explore an obvious question that had not been previously addressed in our past work. Namely, could conventional supports be utilized instead of spinel oxides as a carrier for the transition metal(s)? Although the reaction mechanism proposed in a previous quarterly report for the spinel oxide-supported transition metal catalysts would predict not, the question nevertheless needed to be addressed. It was determined that conventional supports are inferior to the spinel oxides used in our past work even if a variety of oxide promoters are introduced onto the surface. It was observed that these catalysts do enhance the production of iso-alcohols; for example, isobutanol is produced in addition to ethanol and n-propanol. However, more optimization work would be needed to obtain alcohol yields and higher alcohol selectivities competitive with those obtained thus far with the spinel oxide supported catalysts. Work planned for the next quarter is designed to complete the first round of optimization of the transition metal on spinel oxide support catalysts and will be executed as described in the 12th Quarterly Report. Specifically, a final Latin square experimental designed set is planned to complete the bracketing of catalyst formulation, preparation, and pretreatment procedures. This will be followed by a five-variable factorial or face-centered cube designed set of experiments to further characterize the response surface and locate optimum performance.

B. Task 3: Engineering Studies

The slurry reaction system was successfully started up using a standard Cu/Zn/Al methanol catalyst (CCI #6341) to test the performance of the system and demonstrate our ability to obtain quality kinetic data. The results of these tests showed: 1) tetraglyme (tetraethylene glycol dimethyl ether) is not a good solvent for the process, 2) using dodecane as a solvent, we were able to obtain quality data which gave us a good material balance, and 3) a kinetic model developed from the dodecane data was able to predict methanol productivity reported by other researchers. We plan to perform a few more tests using different activation techniques before testing the catalyst developed under Task 2 of this effort.

The methanol catalyst was tested for 216 hours in the slurry reactor using tetraglyme as the solvent. At 240°C, with stoichiometric H₂:CO feed, pressure

between 750 and 950 psig and GHSV of 1000 SI/kg-hr, the methanol productivity dropped from 0.04 g/g-hr to around 0.003 g/g-hr in 100 hours. Reactivating the catalyst in situ restored about half of the original activity, but again the productivity quickly dropped off to less than 0.005 g/g-hr.

The methanol catalyst was tested for 806 hours in the slurry reactor using dodecane as the solvent. During this test, our dodecane material balance was excellent and the elemental carbon balance (excluding dodecane) was typically within ten percent.

Two experimental designed sets were run during this test along with several center-points in order to determine the catalyst's deactivation rate. The first designed set was developed to determine the effects of temperature and partial pressure of hydrogen and carbon monoxide. This set indicated that methanol was inhibiting the reaction even though we were operating far from equilibrium, so a second set was run to determine the effect of methanol inhibition. Regression of the data sets produced a model for the production rate of methanol that provided a good fit of the experimental data. The model was also able to predict the results of literature and plant data with reasonable accuracy. The catalyst deactivated at a rate of 0.28%/hour in this test, which is over an order of magnitude lower than the rate of deactivation in the test using tetraglyme as the solvent.

V. CHANGES

There were no contract changes during this quarter.

VI. FUTURE WORK

Work during the next quarter will continue on Tasks 2 and 3, as described in the schedule of Section II.

Task 2 work on heterogeneous catalysts for alcohol production will continue. This work will include the exploration of novel types of heterogeneous catalysts for the conversion of syngas to oxygenates.

Work on Task 3 will involve economic and engineering evaluations as required to support the chemical investigations. It will also involve the study of slurry-catalyzed systems for the production of fuel alcohols.

APPENDIXES

By J. G. Hippler and G. R. Sheffer

Appendix A. USE OF CODE SYSTEM

A code system is being used in this report and throughout the contract period to identify proprietary data or information which may be the subject of future patents. The code system consists of three classifications, each member of which is assigned a number.

Category A encompasses additives, such as ligands, metal complexes, or salts, which apparently function as catalyst promoters.

Category C consists of catalysts or co-catalysts.

Category S includes solvents for catalytic reactions.

Use of the code system has been approved by the Chief Office of Patent Counsel, U.S. Department of Energy, 9800 South Cass Avenue, Argonne, Illinois 60439.

The following coded information is included in this report:

A131 - A162: Metal catalyst additives

Appendix B. PROCEDURES FOR CATALYST TESTING

Catalyst tests carried out under this contract are assigned reference ID numbers which identify the appropriate researcher and the notebook reference of the experiment.

Procedure B(i)

All catalyst evaluations are performed on a microreactor system designed to operate three 6-milliliter u-shaped fixed-bed reaction tubes simultaneously at pressures of 15-1500 psig, at temperatures between 25 and 400°C, and space velocities between 600 and 6000 hr⁻¹ (STP). This reactor system was described in detail in our Eighth Quarterly Report. The system is capable of automated on-line gas-phase product analysis with post-sampling knock-out pots to collect product for future analysis. Pressure, feed gas composition and velocity, and off-gas sampling may be operated independently for each reaction tube. However, because the tubes utilize a common sandbath, they must be operated at the same reaction temperature. The microreactor system is equipped with an Emergency Shutdown System (ESD) for unattended, overnight operation.

The standard start-up procedure consists of charging the catalyst, generally in powder form, to the outlet leg of a u-shaped 1/4 in. O.D. 304 stainless steel tube. The catalyst is always diluted with an equal volume of 0.5mm glass beads to minimize the pressure drop across the bed. The inlet leg of the u-tube is filled with activated carbon to trap and decompose any metal carbonyl in the feed gas. Glass wool plugs are used to hold all solids in place. The inertness of all non-catalytic materials has been confirmed. The catalysts are activated using H₂/N₂ gas mixtures at atmospheric pressure in a modified gas chromatograph. The tubes are then placed into the microreactor system. The system is subsequently pressurized with feed gas. The absence of gas leaks is verified with soap solution. After reaction pressure is established, the feed gas flow rate is set and measured. The sandbath temperature is then increased to the desired setpoint. Finally, the off-gas analysis system is activated to provide sampling of the reactor effluent for each reactor tube every four hours.

Appendix C. PROCEDURES FOR PRODUCT ANALYSIS

Procedure C(f)

All product analyses are completed in the gas phase using heated lines to transfer reactor effluent samples. A single Varian 3700 gas chromatograph equipped with two detectors is used for off-gas analysis. Inorganics (H_2 , N_2 , CO, and CO_2) are separated on a 1/8 in. x 10 ft. 80/100 mesh Carbosieve S-2 column purchased from Supelco and are measured by a thermal conductivity detector. All organic products are resolved on a 1/8 in. x 12 ft. 80/100 mesh Tenax column obtained from Alltech and are measured using a flame ionization detector. The Tenax column has been calibrated on an absolute weight basis using quantified mixtures of C_1 - C_6 normal hydrocarbons, normal and branched alcohols, and normal aldehydes. Argon is used as the carrier gas for both columns. The following parameters are used for the GC oven and the two columns and detectors:

Temperature ramp: 50°C to 225°C at 8°C/min with a
10 minute hold at the upper temperature

<u>Column</u>	<u>Flow Rate</u>	<u>Injector Temperature</u>
Tenax	20 sccm	220°C
Carbosieve (sample)	20 sccm	170°C
Carbosieve (reference)	20 sccm	170°C

<u>Detector</u>	<u>Temperature</u>	<u>Sensitivity</u>	<u>Attenuation</u>	<u>Other</u>
TCD	200°C	5.0 mV	4X	Filament Temp. = 350°C
FID	250°C	10-10	8X	H_2 flow = 30 sccm Air flow = 300 sccm

Appendix D. TECHNICAL AND EXPERIMENTAL DATA

TABLE OF CONTENTS

I. TASK 2: Catalyst Research	13
A. Direct Syngas Conversion by Heterogeneous Catalysts	13
1. Introduction	13
2. Catalyst Preparation and Characterization	13
3. Catalyst Testing	14
4. Catalytic Results	14
5. Future Work	24
B. Task 2 Summary	25
II. TASK 3: Engineering Research	25
A. Reaction Engineering Studies	25
1. Introduction	25
2. Results with Tetraglyme Solvent.....	25
3. Results with Dodecane Solvent	28
B. Task 3 Summary	50

I. TASK 2: Catalyst Research

A. Direct Syngas Conversion by Heterogeneous Catalysts

1. Introduction

Work continues on optimization of higher alcohol catalysts consisting of transition metals supported on metal oxides with the spinel structure. Our work this quarter was designed to compare conventional supports with spinel oxides as a carrier for the transition metal catalyst components.

2. Catalyst Preparation and Characterization

Catalyst Preparation: Except as noted, catalysts this quarter consisted of a support, oxide promoters, alkali promoters, and transition metals. Catalysts were prepared and assembled as follows. The support was either vendor-supplied or prepared in-house by precipitation of an aqueous solution of the support salt with alkali carbonate solution. The precipitate was subsequently calcined to yield the support material. A listing of the supports used, their origin, and their physical properties is provided in Table 1.

Table 1. Origin and Physical Properties of Catalyst Supports Used.

<u>Support Element</u>	<u>Origin</u>	<u>Surface Area</u>	<u>Pore Volume</u>
A135	1-GRS-29	81 m ² /g	1.67 ml/g
A138	1-GRS-68	78 m ² /g	0.89 ml/g
A143	Calsicat-E149SC	100 m ² /g	0.73 ml/g
A144	1-GRS-94	28 m ² /g	0.90 ml/g
A148	1-GRS-105	77 m ² /g	1.11 ml/g
A157	Criterion-980SG	72 m ² /g	1.41 ml/g

The oxide promoters, i.e., elements whose oxides are non-reducible under typical syngas reaction conditions, were introduced by aqueous incipient wetness impregnation of a water-soluble salt. Calcination at 400°C yields the oxide on the support surface. Next, the support was reimpregnated to incipient wetness with an aqueous solution containing the transition metals to be supported along with the alkali promoter. The alkali formate and metal nitrate salts were used for these impregnations. The amount of metal and other promoters impregnated was determined with respect to a desired surface layer coverage of the components by calculating the moles of element needed

based on the metallic radius of the element (for transition metals) or the molar weighted ionic radius for the element and oxygen (for oxide or alkali elements) and the surface area of the support used.

Catalyst Characterization: Surface areas of all supports were measured using nitrogen adsorption isotherms. The pore volume of each support was found by measuring the amount of water needed to bring the support to incipient wetness. Catalyst densities were determined by measuring the volume in a graduated tube of a specified weight of catalyst.

3. Catalyst Testing

All catalysts were evaluated using Procedure B(i) of Appendix B, and products were analyzed using Procedure C(f) of Appendix C. Before syngas reaction, catalysts were activated by passing a 5% hydrogen in nitrogen gas mix over the catalyst at 400°C for 4 hours using a temperature ramp of 2°C/min. The system was then pressurized with syngas containing an equimolar concentration of carbon monoxide and hydrogen to 1100 psig. The temperature and the syngas flow rate were then adjusted to the desired levels. The reaction product in most cases consisted exclusively of normal paraffins and alcohols.

4. Catalytic Results

Over the past three quarters, our experimentation has been concerned with the optimization of spinel oxide-supported transition metal catalysts. An interesting question for consideration was whether equivalent catalysts could be developed by surface-doping conventional supports with various metal oxide promoters. A five-variable, four-level, Hyper-Greco-Latin Square was designed to explore this possibility, as recorded in Table 2 below. Only the elements used were varied in this set of catalysts; transition metal and alkali were incorporated at levels similar to those in the spinel oxide catalysts. It was intended that the composition of the new catalysts could be further optimized if the approach appeared to have merit.

Table 2. Transition Metals on Metal Oxide-Promoted Conventional Supports.
 Designed Set 1: Hyper-Greco-Latin Square Design to Examine Catalyst
 Formulation.

	<u>Support</u>	<u>Oxide Promoter</u>	<u>Major Metal</u>	<u>Minor Metal</u>	<u>Alkali Promoter</u>
Level 1	A144	A154	A153	A159	A160
Level 2	A157	A146	A131	A133	A149
Level 3	A148	A136	A158	A132	A151
Level 4	A135	A155	A132	A131	A152

Sixteen catalysts were prepared for this experimental designed set, with compositions listed in Table 3. The metal loadings were maintained at 1/3 monolayer for the major metal and 1/9 monolayer for the minor metal. An alkali coverage of 2.0×10^{18} atoms/m² was used for all catalysts. The oxide promoters were incorporated at a level of 1/3 monolayer.

Table 3. Transition Metals on Metal Oxide-Promoted Conventional Supports.
 Designed Set 1: Catalyst Compositions.

<u>Preparation Notebook #</u>	<u>Support</u>	<u>Oxide Promoter</u>	<u>Major Metal</u>	<u>Minor Metal</u>	<u>Alkali Promoter</u>
1-GRS-104	A157	A146	A153	A131	A151
1-GRS-105	A148	A146	A132	A159	A149
1-GRS-106	A157	A155	A158	A159	A152
1-GRS-107	A135	A155	A153	A132	A149
1-GRS-108	A144	A155	A132	A133	A151
1-GRS-109	A135	A146	A158	A133	A160
1-GRS-110	A148	A154	A158	A132	A151
1-GRS-111	A157	A154	A131	A133	A149
1-GRS-112	A144	A146	A131	A132	A152
1-GRS-113	A144	A136	A158	A131	A149
1-GRS-114	A148	A155	A131	A131	A160
1-GRS-115	A135	A154	A132	A131	A152
1-GRS-116	A135	A136	A131	A159	A151
1-GRS-117	A157	A136	A132	A132	A160
1-GRS-118	A144	A154	A153	A159	A160
1-GRS-119	A148	A136	A153	A133	A152

The behavior of the individual catalysts is summarized in Table 4, and the analysis of the Latin Square is presented in Table 5. A simple series of pluses and minuses has been used to indicate the magnitude of influence of each of the variables on the grand average of all responses. The grand average as well as the approximate magnitude of a single plus/minus sign is indicated for each category. Note that three was the maximum number of pluses or minuses given. The maximum result predicted for each category is also provided in the tables. Activity was evaluated on a support surface area-normalized basis as well as a volume basis because of the relatively wide range in surface area (28 to 81 m²/g) of the supports examined.

Table 4. Transition Metals on Metal Oxide-Promoted Conventional Supports.
 Designed Set 1: Catalyst Performance Data.
 Conditions: 310°C, 1100 psig, SV = 50 cc/g cat/min, H₂/CO = 0.5

Catalyst	Alcohol Selec. (wt%)			Alcohol Yield	
	total	(C ₂ +)*	(i-C ₄)*	(lb/ft ³ /hr)	(g/g cat/hr)
1-GRS-104	32	30	4	0.1	0.001
1-GRS-105	50	15	5	0.2	0.003
1-GRS-106	93	8	4	2.0	0.059
1-GRS-107	57	53	1	0.9	0.013
1-GRS-108	92	3	1	1.0	0.016
1-GRS-109	86	15	6	0.2	0.007
1-GRS-110	16	38	3	0.1	0.001
1-GRS-111	0	0	0	0.0	0.000
1-GRS-112	33	6	2	0.3	0.004
1-GRS-113	67	2	0	0.1	0.002
1-GRS-114	69	4	1	3.0	0.043
1-GRS-115	75	8	4	0.3	0.007
1-GRS-116	45	6	0	0.1	0.001
1-GRS-117	95	1	0	0.6	0.022
1-GRS-118	63	11	6	0.1	0.002
1-GRS-119	96	1	0	1.4	0.023

*weight fraction of higher (C₂⁺) alcohols or isobutanol (i-C₄) in overall alcohol product.

Table 5. Transition Metals on Metal Oxide-Promoted Conventional Supports.
 Designed Set 1: Chemical Reactivity Responses Relative to the HGL Square
 Grand Average.

<u>Variable</u>	<u>Level</u>	Alcohol selectivity <u>(wt%)</u>	C ₂ + alc. selectivity <u>(wt%)</u>	Alcohol rate <u>(g/m²/hr)</u>	Alcohol rate <u>(lb/ft³/hr)</u>
Support	A144	+	--	0	--
Support	A157	-	-	+	0
Support	A148	-	+	0	+++
Support	A135	+	++	----	--
Oxide Promoter	A154	----	0	----	----
Oxide Promoter	A146	----	+	----	----
Oxide Promoter	A136	+++	----	-	0
Oxide Promoter	A155	+++	+	+++	+++
Major Metal	A153	0	+++	-	0
Major Metal	A131	----	--	0	++
Major Metal	A158	+	+	++	0
Major Metal	A132	+++	--	0	-
Minor Metal	A159	+	-	++	0
Minor Metal	A133	++	--	+	0
Minor Metal	A132	----	+++	----	-
Minor Metal	A131	0	0	0	++
Alkali Promoter	A160	+++	-	0	+++
Alkali Promoter	A149	----	+	----	----
Alkali Promoter	A151	----	++	-	----
Alkali Promoter	A152	+++	--	+++	+++
Grand Average		61 (+/- = 5%)	13 (+/- = 25%)	19E-5 (+/- = 20%)	0.7 (+/- = 50%)
Maximum Predicted		126	55	96E-5	3.3

Unlike the spinel oxide-supported transition metal catalysts, the catalysts prepared using metal oxide-promoted conventional supports resulted in the formation of a large proportion of iso-alcohols, particularly isobutanol, in the higher alcohol product. In some cases isobutanol constituted as much as 50% of the higher alcohol product. Overall, the catalysts prepared were not as active as the spinel oxide-based catalysts although the alcohol selectivity was better. When the results are scrutinized, the following observations become apparent with respect to each of the elements examined:

1. Support: Compared with the other variables examined, the support had less influence on catalyst performance. A135, the most basic support utilized, was the most detrimental toward alcohol yield. A144, A157, and A148 were similar in performance, except that A144 decreased the higher alcohol selectivity to a greater extent than the other two. Since support A144 had a relatively low surface area, future experiments should look at impregnating it on a A148 or A157 support surface.
2. Oxide Promoter: All the metal oxide support surface promoters studied except A155 had a very negative effect on alcohol yield. A136 did however have a positive effect on alcohol selectivity, particularly for methanol.
3. Major Metal: Of the transition metals examined under this variable, A158 had the greatest effect on alcohol activity. A132, the transition metal of greatest interest in the spinel oxide catalysts, had the greatest positive influence on alcohol selectivity, but not for higher alcohol formation.
4. Minor Metal: A133 and A159 had a positive effect on alcohol selectivity and yield. Interestingly A132 when added in small amounts to the major metal has a very negative effect on alcohol formation, although it does serve to increase the proportion of higher alcohols.
5. Alkali Promoter: Unlike the spinel oxide catalysts, A152 was the most effective promoter. A149 and A151 which were both satisfactory in the spinel oxide case are clearly inferior when using conventional supports, although both resulted in increased higher alcohol selectivities.

Overall, the maximum alcohol yield predicted was 96×10^{-5} g/m²/hr or 3.3 lb/ft³/hr at 310°C and a GHSV=4000 hr⁻¹. However, the combination of elements that would give the maximum alcohol yield is predicted to give a higher alcohol selectivity of only 7 wt%. A combination of elements (A148, A155, A158, A131, A151) that would provide a higher alcohol selectivity of 30 wt%, the minimum acceptable higher alcohol selectivity,

would result in an alcohol yield of only 35×10^{-5} g/m²/hr (approx. 1.2 lb/ft³/hr). In other words, the use of conventional supports is more advantageous for the formation of methanol than higher alcohols. The use of oxide promoters to promote the support surface was generally a disappointment except for A155.

As noted previously, a considerable amount of isobutanol was observed in the higher alcohol product. Perhaps it would be possible to increase the higher alcohol selectivity, especially that of isobutanol, and still achieve an acceptable overall alcohol yield by increasing the reaction temperature. A second designed set was created to explore the effect of using a higher reaction temperature as well as to continue screening other supports and metal oxide promoters.

Specifically, a 4x3 Hyper-Greco-Latin Square experimental set was designed, as shown in Table 6. In this designed set, supports A138 and A143 are compared with supports A148 and A157, which were the best performers in the first designed set; the best metal candidates from designed set 1, namely A133, A158, A159, and A131, are further evaluated individually and in alloys; A144 and similar elements are explored as promoters; and A155 and similar elements are further tested as metal oxide support surface promoters.

Table 6. Transition Metals on Metal Oxide-Promoted Conventional Supports.
Designed Set 2: Further Examination of Catalyst Formulation at Higher Reaction Temperature.

	Major <u>Metal</u>	Minor <u>Metal</u>	<u>Support</u>	A155-Type <u>Oxide Promoter</u>	A144-Type <u>Oxide Promoter</u>
Level 1	A131	A131	A148	A141	none
Level 2	A158	A158	A143	A156	A162
Level 3	A133	A133	A138	A161	A144
Level 4	A159	A159	A157	A155	A145

Sixteen catalysts were prepared for designed set 2, as listed in Table 7. The concentration of transition metals on the support was maintained at 1/9 monolayer for the major metal and 1/18 monolayer for the minor metal. Both mono- and bi-metallic catalysts were studied. The concentration of A144 or A144-type promoter was 1/6 monolayer, while that of the metal oxide surface promoter A155 or A155-type elements was 1/3 monolayer as the oxide. The alkali promoter A152 was added to all catalysts at a level of 2.0×10^{18} atoms/m².

Table 7. Transition Metals on Metal Oxide-Promoted Conventional Supports.
Designed Set 2: Catalyst Compositions.

Preparation <u>Notebook #</u>	Major <u>Metal</u>	Minor <u>Metal</u>	<u>Support</u>	A155-Type <u>Oxide Promoter</u>	A144-Type <u>Oxide Promoter</u>
5-GRS-25	A131	A131	A148	A141	none
5-GRS-26	A131	A158	A143	A161	A145
5-GRS-27	A131	A133	A138	A155	A162
5-GRS-28	A131	A159	A157	A156	A144
5-GRS-29	A158	A131	A143	A156	A162
5-GRS-30	A158	A158	A148	A155	A144
5-GRS-31	A158	A133	A157	A161	none
5-GRS-32	A158	A159	A143	A141	A145
5-GRS-33	A133	A131	A143	A161	A144
5-GRS-34	A133	A158	A157	A141	A162
5-GRS-35	A133	A133	A148	A156	A145
5-GRS-36	A133	A159	A143	A155	none
5-GRS-37	A159	A131	A157	A155	A145
5-GRS-38	A159	A158	A143	A156	none
5-GRS-39	A159	A133	A143	A141	A144
5-GRS-40	A159	A159	A148	A161	A162

The results for the individual catalysts are shown in Table 8, while the analysis of the Latin Square is summarized, using pluses and minuses as outlined previously, in Table 9. Since the range of surface areas of the supports used was relatively narrow (72 to 100 m²/g), catalyst activity was judged only on a weight or volume-normalized basis.

Table 8. Transition Metals on Metal Oxide-Promoted Conventional Supports.
 Designed Set 2: Catalyst Performance Data.
 Conditions: 380°C, 1100 psig, SV = 100 cc/g cat/min, H₂/CO = 0.5

Catalyst	Alcohol Selec. (wt%)			Alcohol Yield	
	total	(C ₂ +)*	(i-C ₄)*	(lb/ft ³ /hr)	(g/g cat/hr)
5-GRS-25	52	8	7	4.2	0.060
5-GRS-26	43	27	11	4.6	0.073
5-GRS-27	68	32	16	4.6	0.103
5-GRS-28	36	14	10	0.5	0.011
5-GRS-29	16	12	3	0.2	0.003
5-GRS-30	58	20	17	5.8	0.075
5-GRS-31	21	63	33	0.4	0.007
5-GRS-32	35	49	9	3.2	0.077
5-GRS-33	64	19	7	5.2	0.083
5-GRS-34	24	73	31	0.5	0.009
5-GRS-35	34	17	4	2.8	0.044
5-GRS-36	17	71	21	0.4	0.006
5-GRS-37	37	27	6	1.5	0.036
5-GRS-38	31	35	5	1.0	0.023
5-GRS-39	8	50	9	0.2	0.003
5-GRS-40	54	20	17	4.1	0.059

*weight fraction of higher (C₂⁺) alcohols or isobutanol (i-C₄) in overall alcohol product.

Table 9. Transition Metals on Metal Oxide-Promoted Conventional Supports.
 Designed Set 2: Catalyst Chemical Reactivity Responses Relative to the HGL
 Grand Average.

<u>Variable</u>	<u>Level</u>	<u>Alcohol selectivity (wt%)</u>	<u>C₂+ alc. selectivity (wt%)</u>	<u>Alcohol Yield (g/g/hr)</u>	<u>Isobutanol Yield (g/g/hr)</u>
Major Metal	A131	++	--	+++	++
Major Metal	A158	-	0	0	+
Major Metal	A133	0	++	-	---
Major Metal	A159	-	0	---	-
Minor Metal	A131	+	---	+	---
Minor Metal	A158	0	+	0	+
Minor Metal	A133	-	+	0	0
Minor Metal	A159	0	+	0	0
Support	A148	++	---	+++	+++
Support	A143	---	+	---	---
Support	A138	++	0	+++	+++
Support	A157	-	++	---	---
A155-Type Oxide	A141	-	++	0	-
A155-Type Oxide	A156	-	--	---	---
A155-Type Oxide	A161	+	0	++	++
A155-Type Oxide	A155	+	0	++	+++
A144-Type Oxide	none	-	++	---	---
A144-Type Oxide	A162	0	0	0	+++
A144-Type Oxide	A144	+	-	0	0
A144-Type Oxide	A145	0	0	+++	0
Grand Average		37	34	0.054	0.006
		(+/- = 15%)	(+/- = 15%)	(+/- = 10%)	(+/- = 15%)
Maximum Predicted		78	85	0.157	0.019

On examining the results listed in Table 8, the following observations become apparent with respect to each of the variables studied:

1. Major Metal: Interestingly, A131 appeared to be better than A158, which was the best metal in the first designed set. This may be a result of a higher activation energy for methanol formation for A131 relative to A158 since it is observed that A131 is primarily a methanol synthesis metal and results in low higher alcohol production. A133 had the greatest effect on higher alcohol selectivity but with a small negative influence on alcohol yield. A159 appeared to be the least desirable of the metals tested.
2. Minor Metal: None of the co-metals used appeared to have a great effect on catalyst performance, unlike in the first designed set. As with the results for the Major Metals, A131 still appeared to be somewhat superior in terms of increasing the yield, but again at the expense of higher alcohol formation.
3. Support: A148 and A138 were more beneficial than A157 and A143 with respect to alcohol selectivity and yield. However, A138 did not have a detrimental effect on higher alcohol selectivity while A148 did. An overall ranking of $A138 > A148 > A157 > A143$ is apparent.
4. A155-Type Compounds: A155 and A161 were equivalent in catalytic performance. None of the three other elements tested were superior to A155. A155 and A161 resulted in increased yields with very little effect on product selectivities.
5. A144-Type Compounds: Compared with the case of using none at all, all three elements tested were superior in terms of alcohol yield. However, the yield increase was for primarily methanol since the effect on higher alcohol selectivity was inferior to the case using no promoter at all.

Overall, the results of the second experimental designed set indicate that catalyst with an alcohol yield of 0.157 g/g/hr or approximately 7 lb/ft³/hr should be possible at 380°C and GHSV=6000 hr⁻¹. However, as in the first designed set, the selectivity to higher alcohols using the most preferred elements from a yield standpoint would be low, about 10 wt%. Conversely, a more suitable elemental combination from a higher alcohol selectivity vantage, such as A131, A133, A138, A141, and A162, would result in a higher alcohol selectivity of 30 wt% (the minimum acceptable), but with an alcohol yield of only 0.08 g/g/hr or approximately 4 lb/ft³/hr. In other words, even though overall rates somewhat comparable to the spinel oxide-supported catalysts (5-15

lb/ft³/hr to date) are achievable at 380°C, the necessary selectivity to higher alcohols is not. Thus it appears that the spinel oxide supports are truly synergistic for the formation of higher alcohols with transition metals.

5. Future Work

Future work in the next quarter will begin where the work reported in the 12th quarter ended. In order to finish the bracketing or choosing of catalyst formulation and preparation variables for the spinel oxide-supported transition metal catalysts in the upcoming quarter, an eighth 4x3 Hyper-Greco-Latin Square designed set will be executed. It is anticipated that this designed set will be followed by a 5-variable factorial or face-centered cube design to map the response surface and expose the nature of the interactions of the primary variables. The eighth Latin square is intended to further bracket the optimum calcination temperature, further bracket the A132 loading, study the effect of spinel precursor pH and temperature of precipitation, examine the influence of reaction temperatures over the range of 250 to 290°C, examine other methods of A132 impregnation, and evaluate other basic elements in addition to the alkalis, as suggested by designed set 6 summarized in the 12th Quarterly Report.

B. Task 2 Summary

Work continues on optimization of higher alcohol catalysts consisting of transition metals supported on metal oxides with the spinel structure. Our work this quarter was designed to explore an obvious question that had not been previously addressed in our work. Namely, could conventional supports be utilized instead of spinel oxides as a carrier for the transition metal(s)? Although the proposed reaction mechanism presented in a previous quarterly for the transition metal(s) spinel oxide supported catalysts would predict not, the question nevertheless needed to be addressed. It was determined that conventional supports are inferior to the spinel oxides used in our past work even if a variety of oxide promoters are introduced onto the surface. It was observed that these catalysts do enhance the production of iso-alcohols, for example, isobutanol in addition to ethanol and n-propanol. However, more optimization work would be needed to obtain alcohol yields and higher alcohol selectivities competitive with those obtained thus far with the spinel oxide supported catalysts. Work planned for the next quarter is designed to complete the first round of optimization of the transition metal on spinel oxide support catalysts and will be executed as described in the 12th Quarterly Report. Specifically, a final Latin square experimental design to complete the bracketing of catalyst formulation, preparation, and pretreatment procedures is planned. This will be followed by a five-variable factorial or face-centered cube designed set of experiments to further characterize the response surface and location of optimum levels.

II. TASK 3: Engineering Research

A. Reaction Engineering Studies

1. Introduction

Two series of tests were completed on the conversion of syngas to methanol using CCI #6341 Cu/Zn/Al catalyst in the slurry reactor. These tests were done in order to 1) test the operation of the reaction system under reaction conditions, 2) demonstrate our ability to obtain kinetic information from the reactor, 3) determine a good solvent for use in future testing, and 4) develop a satisfactory *in situ* catalyst reduction technique. We have satisfied our first three objectives. The reaction system performed very well under reaction conditions. The kinetic data generated from the reactor was modeled and fit some literature values reasonable well. We also demonstrated that methanol has a strong inhibiting effect on the reaction even far from equilibrium. Dodecane appears to be a good solvent; tetraglyme is not. We still need to run a few more tests using different activation techniques to determine catalyst sensitivity to activation procedure. After these tests are completed, the higher alcohol catalyst developed under Task 2 will be tested in the slurry reactor.

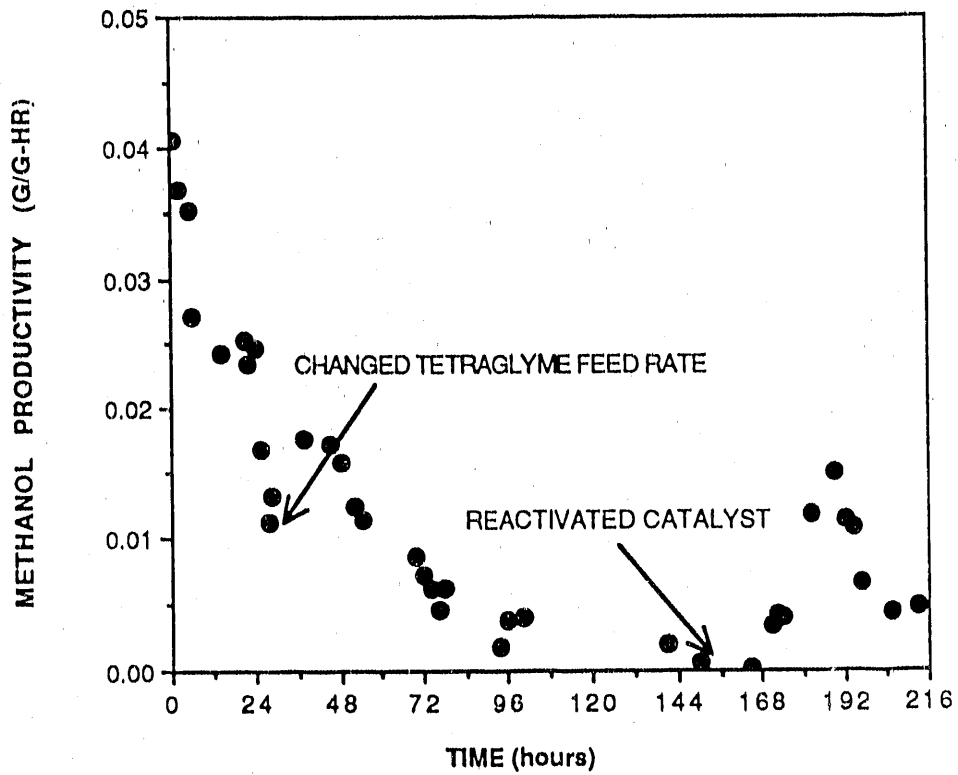
2. Results With Tetraglyme Solvent

The two-liter slurry reactor (which was described in a previous report) was charged with 25.9 grams of CCI #6341 Cu/Zn/Al catalyst which was crushed and sieved to 75 - 150 microns. Tetraglyme (tetraethylene glycol dimethyl ether) was added to the reactor and the catalyst was activated *in situ*. The catalyst was activated by feeding 150 sccm of a 1:1 H₂:N₂ mixture to the reactor which was at 100 psig while ramping the temperature from 150°C to 250°C over a 24 hour period. The hydrogenation reaction was carried out by feeding 450 sccm of a 2:1 H₂/CO mixture to the reactor which was at 240°C and 750 to 1000 psig. In order to keep a constant liquid level, tetraglyme was fed to the reactor at 60 ml/hr for the first 24 hours and 20 ml/hr for the rest of the test.

Figure 1 shows the results of this test. The initial methanol productivity was 0.04 g-methanol/g-catalyst-hr. The methanol productivity quickly dropped off to less than 0.002 g/g-hr in about 100 hours. There was a temporary decrease in the methanol productivity after 24 hours when the tetraglyme feed rate was decreased because of the accumulation of methanol in the liquid phase. After 168 hours, the CO was turned off and the catalyst was reactivated using the procedure described above. Reactivating the catalyst increased the methanol productivity to 0.015 g/g-hr, but the productivity quickly decreased and the test was terminated after 216 hours.

FIGURE 1

PRODUCTIVITY OF METHANOL
USING TETRAGLYME AS SOLVENT



CONDITIONS:

240°C

750-1000 PSIG

2:1 H₂:CO

GHSV = 1000 SL/KG-HR

3. Results With Dodecane Solvent

The two-liter slurry reactor was charged with 25.6 grams of 75 - 150 micron CCI #6341 catalyst. Dodecane was added to the reactor and the catalyst was activated by feeding 200 sccm of a 1:3 H₂/N₂ mixture to the reactor which was at 200 psig while ramping the temperature from 150°C to 240°C over a 24 hour period. The pressure was increased to 750 psig and 200 sccm of H₂ was fed for four hours. The hydrogenation reaction was then started by feeding 450 sccm of a 2:1 H₂/CO mixture to the reactor which was at 240°C and 750 psig. In order to keep a constant liquid level, dodecane was fed to the reactor at 30 ml/hr for the first four days and 15 ml/hr for the rest of the test.

Both the gas and the liquid effluent from the reactor were analyzed using the gas chromatograph method discussed in the previous quarterly report. In some samples, the liquid sample contained both an organic and an aqueous phase which were separated and analyzed separately. The results from the analysis of the the gas and both liquid phases are presented in Tables 10 - 12. Table 13 presents the operating conditions of the reactor at each sample time. Table 14 presents the calculations of the methanol productivity as well as the material balance for the dodecane and the elemental carbon. Table 15 shows the production rate of methanol, methane, and carbon dioxide along with the partial pressures of each of the components for each sample.

The catalyst required about 60 hours to lose its initial hyperactivity after activation. Figure 2 shows the initial methanol productivity for the first 200 hours of operation. During this time, the reaction was at 240°C and 750 psig with 450 sccm of a 2:1 H₂/CO feed (GHSV = 1050 SI/hr-Kg). After 160 hours, the first of two designed sets of experiments were started.

The first designed set was developed in order to determine the effects of temperature, pressure, and feed ratio on the productivity. The conditions used for these tests are shown in Figure 3 and the results of these tests are shown in Table 15. Multiple regression of the methanol productivity rate produced the expression

$$\text{PRODUCTIVITY (g/g-hr)} = e^{(-0.445-8810/RT)} \langle \text{H}_2 \rangle^{1.018}$$

where $\langle \text{H}_2 \rangle$ is the hydrogen partial pressure in psia. This model provided a good fit of the data, but the low activation energy and first-order effect on hydrogen suggested that there were other important effects were not being considered.

A second designed set was then run to determine the effect of methanol on the reaction rate. In this set the temperature and gas feed rate were varied, and methanol was also fed directly to the reactor in three of the runs. The results of this set are summarized in Table 16.

The data in Table 16 show clearly that feeding methanol to the reactor has a strong detrimental effect on the methanol productivity. This was unexpected because the reaction is far from equilibrium at 950 psig with less than ten percent conversion. Regression of the above data showed that the methanol partial pressure inhibits the reaction to the -1.23 power. The partial pressure of methanol can be used even though this is a liquid phase reaction by assuming that the vapor phase is an ideal mixture (the vapor pressure equals the vapor fugacity), and by assuming vapor-liquid equilibrium (the vapor fugacity equals the liquid fugacity).

The equation for the methanol production is shown below.

$$\text{METHANOL PRODUCTIVITY (g/g-hr)} = e^{(27,448-27168/RT)} \langle \text{MeOH} \rangle^{-1.23}$$

$$R^2 = 0.895$$

As expected¹, the activation energy is significantly higher when the methanol inhibition is accounted for. In order to simplify development of the model, a -1 order for methanol inhibition was assumed.

The reaction can be shown to be far from equilibrium by comparing the equilibrium constant with the ratio of the pressures of the product to the reactants. The run which produced the highest methanol partial pressure at the exit is the closest to equilibrium. In this run (Run #3 in Table 16, which is Sample 1-JGHX-21 in Tables 10 - 15), $P_{\text{MEOH}} = 174$ psia, $P_{\text{H}_2} = 521$ psia, and $P_{\text{CO}} = 254$ psia. From this, the ratio is calculated as

$$K_{\text{OBS}} = \frac{(174)}{(521)^2(254)} = 2.56 \cdot 10^{-6} \text{ psi}^{-2} = 5.3 \cdot 10^{-4} \text{ bar}^{-2}$$

which is an order of magnitude away from the $6 \cdot 10^{-3} \text{ bar}^{-2}$ equilibrium constant reported for this reaction at 500K.² The other runs performed during this work were done with at least one-half to one-quarter the methanol partial pressure and correspondingly higher H_2 and CO pressure. Thus, those runs were even further from equilibrium.

The methanol catalyst was shown to decay at a rate of 0.28% per hour. This is shown in Figure 4. This figure shows the methanol productivity of our centerpoint runs (756 psig, 240°C, 2:1 H_2 :CO, 450 sccm) after correcting for the methanol inhibition. The dark points are those which were regressed to determine the deactivation rate.

The data from designed set #1 were then regressed again. This time the catalyst deactivation rate and the methanol inhibition effect were built into the regression. The results from this regression show a big difference from the original regression:

$$\text{PRODUCTIVITY (g/g-hr)} = e^{(3.071-24171/RT-0.002817)} \langle \text{H}_2 \rangle^{2.95} \langle \text{CO} \rangle^{0.74} \langle \text{MeOH} \rangle^{-1}$$

$$R^2 = 0.966$$

The activation energy has increased to 24 Kcal/gmol, which is about what should be expected of this type of reaction, and the reaction is strongly influenced by the hydrogen partial pressure and less by the CO pressure. In order to simplify the model further, a second-order effect was assumed for hydrogen. Regressing the data with this assumption increased the effect of CO to the 0.92 power. Since there were only five conditions used in this designed set, we can take some more liberties with the model without affecting the fit. Therefore, a first-order effect was assumed for CO and the model was regressed one last time to yield the equation

$$\text{PRODUCTIVITY (g/g-hr)} = e^{(6.241-22861/RT-0.002817)} \frac{\langle \text{H}_2 \rangle^2 \langle \text{CO} \rangle}{\langle \text{MeOH} \rangle}$$

This equation is a simple two-parameter model which does an excellent job of correlating our data as well as the data of others.

Figure 5 presents a parity plot which shows how well the above model fits our data. The model not only fits the data from the first designed set, but also fits the data from the second set as well as the outliers which were run at H₂/CO ratios of 0.75:1 and 3:1.

Figure 6 shows a comparison between the precision of the model developed above and published data from other researchers³. The model provides a relatively good fit of the data considering the differences between their experiments and ours. Their work was done gas-phase in a Berty reactor at six times the GHSV, with up to 24:1 H₂/CO, and at pressures as low as 400 psig.

Figure 7 shows that our model does not do quite as well predicting the performance of the LaPorte PDU Unit⁴. Our model predicts only about 25 to 50 percent of the productivity reported in their unit. However, there are many differences between their unit and ours. While we both operate using a mineral oil slurry at comparable temperature and pressure, the PDU unit appears to be using a different and improved catalyst from what we used. The PDU unit also uses 0.7:1 H₂/CO with 13% CO₂ which is not accounted for in the model, and the space velocity in the PDU unit is up to twenty times higher than we used.

The observation of methanol inhibition has interesting effects on the selection of the optimum reactor. Figure 8 shows our model prediction of the LaPorte PDU operation at three different space velocities assuming a tanks-in-series model. This figure shows that around a thirty percent increase in productivity can be achieved from switching the flow pattern from complete back-mixing to three tanks-in-series. Additional

improvement in the flow pattern toward straight plug-flow produces only a marginal increase in productivity. This is interesting because tracer studies in the LaPorte PDU unit show that their reactor operates as 3 to 4 tanks in series⁴.

Figures 9 and 10 present the material balance data over our reactor. Figure 9 shows that the elemental carbon balance is typically within five percent and within 15 percent in almost all cases. Some of the points show a poor material balance because this graph includes all the data and in some cases the reactor was not running at steady-state conditions. Figure 10 shows that we are able to calculate with good accuracy the amount of dodecane in the reactor. The dodecane inventory was calculated by measuring the amount fed and the amount collected. During the run, over 10000 grams of dodecane was fed over 800 hours.

Figure 11 shows the production rate of CO₂ as measured in our second designed set. The production rate was regressed against temperature and methanol partial pressure. The regression shows that the CO₂ production rate was only a function of temperature (activation energy = 16344 cal/gmole) and not methanol concentration.

Figure 12 shows the production rate of methane as measured in our second designed set. As with the CO₂, the production rate was regressed against temperature and methanol partial pressure. Again, the regression shows that the methane production rate was only a function of temperature (activation energy = 32228 cal/gmole). Thus, we can conclude that the methane and the CO₂ are not being produced from the methanol.

REFERENCES

1. Cropley, J. B., "Systematic Errors in Recycle Reactor Kinetic Studies", *Chem. Eng. Prog.* **83**, 46-51, 1987
2. Chinchon, C. G., et. al., "Synthesis of Methanol Part 1. Catalysts and Kinetics", *Applied Catalysis*, **36** 1-65, 1988.
3. Bos, A. N. R., Borman, P. C., Kuczynski, M., and Westerterp, K. R., "The Kinetics of the Methanol Synthesis on a Copper Catalyst: an Experimental Study", *Chem. Eng. Sci.* **44**, 2435-2449, 1989.
4. Studer, D. W., Brown, D. M., Henderson, J. L., and Hsiung, T. H., "Status of the Development of Methanol Synthesis by the LPMEOH* Process", Proceedings of the Indirect Liquefaction Contractors' Review Meeting, November 13-15, 1989.

Table 10. Off-Gas Analyses, Mole Percent.

SAMPLE REF.	CO HUN	HE	H2	CO2	C2H6	H2O	MECH	ETOH	I-PROH	N-PROH	N2	CO	O14
I-JCHX-18B	0	0.000	40.175	0.321	0.047	0.171	0.000	0.000	0.000	0.000	59.286	0.000	
I-JCHX-18C	0	0.000	77.724	0.082	0.080	0.059	0.000	0.000	0.000	0.000	22.076	0.000	
I-JCHX-18D	0	0.010	60.093	0.455	0.015	0.363	14.316	0.004	0.000	0.000	3.174	21.568	
I-JCHX-18E	0	0.011	60.839	0.306	0.104	0.002	0.943	2.548	0.000	0.000	1.121	28.208	
I-JCHX-18F	262	0.010	62.160	0.375	0.060	0.002	7.254	0.003	0.000	0.000	0.806	29.390	0.000
I-JCHX-18G	263	0.011	61.421	0.556	0.007	0.000	7.047	0.000	0.000	0.000	0.507	30.436	0.015
I-JCHX-18H	267	0.010	62.021	0.365	0.060	0.001	6.172	0.000	0.000	0.000	0.566	30.856	0.005
I-JCHX-18I	0	0.009	62.550	0.477	0.003	0.002	5.356	0.000	0.000	0.000	0.441	31.158	
I-JCHX-18J	269	0.009	62.550	0.477	0.003	0.002	5.356	0.000	0.000	0.000	0.441	31.158	0.005
I-JCHX-18K	0	0.009	63.411	0.466	0.006	0.002	4.075	0.000	0.000	0.000	0.487	31.526	
I-JCHX-18L	0	0.007	61.944	0.417	0.000	0.004	4.397	0.000	0.000	0.000	0.603	32.606	
I-JCHX-20A	0	0.000	63.415	0.504	0.000	0.000	3.859	0.003	0.000	0.000	0.241	31.963	
I-JCHX-20B	0	0.002	63.278	0.502	0.006	0.001	4.268	0.000	0.000	0.000	0.180	31.737	
I-JCHX-20C	0	0.000	63.379	0.369	0.000	0.001	4.174	0.000	0.000	0.000	0.183	31.880	
I-JCHX-20D	0	0.000	61.320	1.563	0.000	0.009	6.303	0.000	0.000	0.000	0.176	30.534	0.055
I-JCHX-20E	0	0.000	61.741	0.533	0.000	0.001	6.579	0.000	0.000	0.000	0.143	30.949	
I-JCHX-20F	0	0.000	62.011	0.683	0.004	0.003	6.283	0.016	0.000	0.000	0.177	30.770	
I-JCHX-20G	0	0.000	62.834	0.675	0.004	0.003	6.122	0.006	0.000	0.000	0.033	30.566	
I-JCHX-20H	0	0.000	62.601	0.508	0.003	0.003	4.639	0.000	0.000	0.001	0.332	31.683	
I-JCHX-20I	0	0.000	62.930	0.513	0.003	0.005	4.735	0.000	0.000	0.000	0.180	31.564	
I-JCHX-20J	0	0.000	62.786	0.499	0.005	0.006	5.044	0.005	0.000	0.000	0.158	31.500	
I-JCHX-20K	315	0.000	62.763	0.542	0.013	0.002	4.602	0.003	0.000	0.000	0.353	31.605	0.117
I-JCHX-20L	318	0.001	62.610	0.526	0.007	0.006	4.533	0.000	0.000	0.000	0.219	31.827	
I-JCHX-20M	320	0.007	75.696	0.318	0.000	0.003	2.838	0.000	0.000	0.000	0.049	20.072	
I-JCHX-20N	323	0.010	76.835	0.421	0.000	0.007	2.743	0.000	0.000	0.000	0.302	19.449	
I-JCHX-20O	333	0.009	70.867	0.239	0.000	0.001	2.685	0.000	0.000	0.000	0.044	20.126	
I-JCHX-20P	340	0.010	68.983	0.396	0.000	0.004	2.481	0.000	0.000	0.000	0.117	27.990	
I-JCHX-20Q	351	0.008	56.187	0.237	0.000	0.000	4.151	0.000	0.000	0.000	0.180	30.248	
I-JCHX-20R	354	0.007	59.644	0.292	0.000	0.000	4.344	0.000	0.000	0.000	0.179	39.523	
I-JCHX-20S	355	0.008	56.777	0.319	0.000	0.000	3.085	0.000	0.000	0.000	0.119	39.688	
I-JCHX-20T	361	0.008	56.110	0.310	0.000	0.000	3.569	0.000	0.000	0.000	0.148	39.853	
I-JCHX-20U	378	0.010	62.061	0.561	0.005	0.005	4.822	0.000	0.000	0.000	0.328	32.094	
I-JCHX-20V	381	0.009	62.371	0.557	0.000	0.002	4.649	0.006	0.000	0.000	0.264	31.926	
I-JCHX-20W	387	0.008	56.755	1.013	0.029	0.000	3.783	0.003	0.000	0.000	0.291	38.024	
I-JCHX-20X	406	0.008	56.113	0.865	0.006	0.001	3.292	0.004	0.000	0.000	0.148	39.452	
I-JCHX-20Y	419	0.008	55.793	0.900	0.000	0.005	3.780	0.012	0.000	0.000	0.185	39.245	
I-JCHX-20Z	431	0.009	55.567	0.925	0.016	0.003	4.285	0.012	0.000	0.000	0.185	38.943	
I-JCHX-20AA	441	0.016	65.655	1.182	0.036	0.005	6.375	0.014	0.000	0.000	0.693	26.476	0.160
I-JCHX-20AB	442	0.012	67.162	1.164	0.006	0.000	6.427	0.000	0.000	0.000	0.181	24.895	0.114
I-JCHX-20AC	452	0.008	66.040	1.389	0.022	0.004	6.251	0.000	0.000	0.000	0.099	23.988	0.199
I-JCHX-20A	454	0.010	67.462	1.371	0.033	0.006	6.547	0.005	0.000	0.000	0.211	24.146	0.209
I-JCHX-20BH	458	0.009	63.314	0.580	0.000	0.002	4.403	0.000	0.000	0.000	0.168	31.508	0.016
I-JCHX-20CH	464	0.009	63.082	0.443	0.000	0.000	4.132	0.000	0.000	0.000	0.188	32.135	0.030
I-JCHX-20DH	472	0.009	63.127	0.547	0.005	0.003	4.154	0.000	0.000	0.000	0.146	31.986	0.024
I-JCHX-20EH	473	0.008	63.100	0.569	0.005	0.000	4.156	0.000	0.000	0.000	0.166	31.936	0.060
I-JCHX-20FH	481	0.008	37.603	1.019	0.034	0.005	6.416	0.022	0.000	0.000	0.248	53.926	0.122
I-JCHX-20GH	491	0.007	33.241	1.522	0.016	0.005	6.091	0.034	0.000	0.000	0.335	58.618	0.129
I-JCHX-20IH	500	0.007	33.866	1.331	0.004	0.003	5.885	0.063	0.000	0.017	0.290	58.484	0.071
I-JCHX-20JH	506	0.014	68.185	0.667	0.013	0.000	6.298	0.003	0.000	0.000	0.000	25.276	0.145
I-JCHX-20JH	511	0.012	69.788	1.655	0.036	0.000	6.931	0.005	0.000	0.000	0.164	21.164	0.224
I-JCHX-20KH	514	0.013	72.502	1.658	0.066	0.015	6.084	0.010	0.000	0.000	0.193	19.198	0.262
I-JCHX-20LH	523	0.011	72.258	1.515	0.068	0.027	6.382	0.000	0.000	0.000	0.155	19.269	0.316
I-JCHX-20MH	526	0.000	72.704	1.644	0.030	0.038	6.470	0.015	0.000	0.000	0.037	18.791	0.273
I-JCHX-20NH	528	0.013	71.827	1.596	0.068	0.037	7.421	0.000	0.000	0.000	0.179	18.764	0.295
I-JCHX-20OH	535	0.015	76.791	0.657	0.069	0.006	6.141	0.034	0.000	0.000	0.000	18.647	0.270
I-JCHX-20PH	537	0.004	65.223	0.534	0.016	0.007	2.938	0.003	0.000	0.000	0.077	31.097	0.099
I-JCHX-20QH	540	0.005	64.271	0.460	0.004	0.004	2.531	0.000	0.000	0.000	0.143	32.520	0.061
I-JCHX-20RH	542	0.005	64.129	0.458	0.017	0.006	2.738	0.004	0.000	0.000	0.144	32.431	0.068
I-JCHX-20SH	549	0.011	61.573	3.220	0.058	0.043	7.092	0.000	0.000	0.000	0.226	27.583	0.213
I-JCHX-20TH	554	0.009	60.992	4.392	0.032	0.019	6.589	0.034	0.007	0.000	0.221	25.450	0.226
I-JCHX-20UH	559	0.010	60.282	2.391	0.013	0.002	9.276	0.004	0.000	0.000	0.110	27.714	0.198
I-JCHX-20VH	566	0.009	60.046	1.877	0.049	0.003	9.177	0.000	0.000	0.000	0.191	28.431	0.218
I-JCHX-20WH	579	0.007	59.642	1.532	0.036	0.009	9.283	0.000	0.000	0.000	0.259	29.047	0.184
I-JCHX-20XH	582	0.008	59.935	1.555	0.019	0.003	8.394	0.000	0.000	0.000	0.297	29.510	0.279
I-JCHX-20XH	579	0.007	59.642	1.532	0.036	0.009	9.283	0.000	0.000	0.000	0.259	29.047	0.184
I-JCHX-20YH	591	0.001	61.238	0.069	0.000	0.000	3.535	0.000	0.000	0.000	0.127	34.905	0.003
I-JCHX-20ZH	595	0.001	64.139	0.127	0.000	0.001	3.185	0.000	0.000	0.000	0.000	32.546	0.001
I-JCHX-20ZH	597	0.002	63.737	0.133	0.000	0.000	3.174	0.000	0.000	0.000	0.109	32.843	0.003
I-JCHX-20AH	606	0.004	62.855	0.362	0.000	0.000	4.598	0.000	0.000	0.000	0.152	32.022	0.007
I-JCHX-20BH	609	0.007	62.968	0.317	0.000	0.003	4.590	0.000	0.000	0.000	0.125	32.045	0.005
I-JCHX-20CH	612	0.007	63.229	0.418	0.000	0.003	4.346	0.000	0.000	0.000	0.109	31.854	0.035
I-JCHX-20DH	618	0.007	62.968	0.401	0.000	0.002	4.810	0.000	0.000	0.000	0.174	31.787	0.032
I-JCHX-20EH	624	0.008	63.795	0.406	0.000	0.000	3.106	0.000	0.000	0.000	0.167	32.510	0.005
I-JCHX-20EH	626	0.003	64.334	0.406	0.000	0.002	2.541	0.000	0.000	0.000	0.145	32.556	0.007
I-JCHX-20FH	630	0.008	63.933	0.408	0.000	0.000	2.303	0.000	0.000	0.000	0.187	33.153	0.007
I-JCHX-20GH	636	0.007	63.992	0.326	0.003	0.003	2.574	0.000	0.000	0.000	0.185	32.886	0.074
I-JCHX-20GH	636	0.007	63.992	0.326	0.003	0.003	2.574	0.000	0.000	0.000	0.185	32.886	0.074
I-JCHX-20JL	645	0.006	64.580	0.372	0.003	0.000	1.877	0.000	0.000	0.000	0.128	33.006	0.027
I-JCHX-20JL	650	0.007	64.057	0.437	0.000	0.005	2.070	0.000	0.000	0.000	0.233	33.136	0.055

Table 11. Organic Layer Analyses, Weight Percent.

SAMPLE REF.	GC RUN	(WEIGHT PERCENT)											
		MEOH	EtOH	I-PROH	T-BUOH	N-PROH	S-BUOH	HIUOH	N-BUOH	DODECANE	GLYME	MISC	
1-JGHX-18B		0.081	0.000	0.123	0.000	0.000	0.000	0.000	0.000	0.000	99.820	0.000	0.000
1-JGHX-18C		0.027	0.000	0.073	0.000	0.000	0.000	0.000	0.000	0.000	99.900	0.000	0.000
1-JGHX-18D		0.030	0.021	0.090	0.000	0.000	0.000	0.000	0.000	0.000	99.881	0.000	0.000
1-JGHX-18E		0.539	0.009	0.019	0.000	0.000	0.000	0.000	0.000	0.000	99.368	0.000	0.000
1-JGHX-18F	273	0.047	0.011	0.018	0.000	0.000	0.000	0.000	0.000	0.000	99.983	0.000	0.000
1-JGHX-18G	278	1.192	0.016	0.020	0.000	0.000	0.010	0.000	0.000	0.000	98.888	0.000	0.000
1-JGHX-18H	276	0.917	0.016	0.028	0.000	0.000	0.012	0.009	0.000	0.011	98.108	0.831	0.073
1-JGHX-18I		0.488	0.007	0.024	0.000	0.000	0.008	0.008	0.000	0.011	98.011	0.852	0.000
1-JGHX-18J	278	0.274	0.000	0.023	0.000	0.000	0.007	0.008	0.000	0.001	99.500	0.000	0.013
1-JGHX-18K		0.213	0.000	0.024	0.000	0.000	0.007	0.008	0.000	0.008	99.730	0.000	0.000
1-JGHX-18L		0.208	0.000	0.024	0.000	0.000	0.009	0.008	0.000	0.007	99.585	0.182	0.000
1-JGHX-20A		0.228	0.012	0.030	0.000	0.000	0.009	0.009	0.000	0.008	99.335	0.378	0.000
1-JGHX-20B		0.184	0.012	0.028	0.000	0.000	0.004	0.009	0.000	0.003	99.781	0.000	0.000
1-JGHX-20C		0.423	0.007	0.021	0.000	0.000	0.008	0.013	0.000	0.011	98.518	0.000	0.000
1-JGHX-20D		1.277	0.019	0.025	0.000	0.000	0.018	0.019	0.004	0.018	98.923	0.000	0.100
1-JGHX-20E		0.044	0.016	0.028	0.000	0.000	0.017	0.014	0.000	0.008	99.531	0.254	0.000
1-JGHX-20F		0.981	0.014	0.028	0.000	0.000	0.014	0.021	0.004	0.005	98.952	0.000	0.000
1-JGHX-20G		0.283	0.031	0.028	0.000	0.000	0.010	0.021	0.003	0.000	99.824	0.000	0.000
1-JGHX-20H		0.287	0.031	0.030	0.000	0.000	0.009	0.021	0.000	0.008	99.834	0.000	0.000
1-JGHX-20I		0.339	0.000	0.029	0.000	0.000	0.009	0.021	0.000	0.013	99.589	0.000	0.000
1-JGHX-20J		0.488	0.010	0.032	0.000	0.000	0.013	0.028	0.000	0.017	99.418	0.000	0.000
1-JGHX-20K	339	0.725	0.013	0.035	0.000	0.000	0.015	0.028	0.000	0.000	99.032	0.000	0.155
1-JGHX-20L	449	0.334	0.008	0.030	0.000	0.000	0.009	0.025	0.003	0.003	99.404	0.000	0.095
1-JGHX-20M	480	0.150	0.000	0.023	0.000	0.000	0.017	0.000	0.000	0.000	99.848	0.000	0.088
1-JGHX-20N	481	0.097	0.000	0.021	0.000	0.000	0.001	0.012	0.000	0.000	99.730	0.000	0.048
1-JGHX-20O	482	0.089	0.000	0.019	0.000	0.000	0.000	0.010	0.000	0.002	99.784	0.000	0.037
1-JGHX-20P	453	0.088	0.000	0.019	0.000	0.000	0.000	0.008	0.000	0.000	99.798	0.000	0.030
1-JGHX-20Q	454	0.139	0.000	0.014	0.000	0.000	0.008	0.000	0.000	0.000	99.780	0.000	0.025
1-JGHX-20R	456	0.133	0.000	0.016	0.000	0.000	0.002	0.007	0.000	0.001	99.782	0.000	0.029
1-JGHX-20S	486	0.119	0.000	0.014	0.000	0.000	0.002	0.008	0.000	0.002	99.788	0.000	0.022
1-JGHX-20T	457	0.183	0.000	0.018	0.000	0.000	0.008	0.000	0.000	0.004	99.702	0.000	0.019
1-JGHX-20U	458	0.839	0.000	0.025	0.000	0.000	0.007	0.018	0.001	0.007	99.168	0.000	0.085
1-JGHX-20V	459	0.770	0.000	0.028	0.000	0.000	0.007	0.019	0.001	0.008	99.017	0.000	0.085
1-JGHX-20W	481	1.251	0.000	0.040	0.012	0.019	0.043	0.011	0.117	0.343	98.343	0.000	0.164
1-JGHX-20X	482	1.581	0.000	0.040	0.031	0.032	0.058	0.022	0.117	0.749	97.749	0.000	0.370
1-JGHX-20Y	484	0.205	0.000	0.041	0.007	0.035	0.040	0.011	0.107	0.330	98.330	0.000	0.165
1-JGHX-20Z	485	0.353	0.000	0.048	0.009	0.017	0.042	0.013	0.110	0.239	98.239	0.000	0.171
1-JGHX-20AA	478	1.444	0.028	0.014	0.038	0.021	0.051	0.017	0.168	0.157	98.157	0.000	0.128
1-JGHX-20AB	478	1.387	0.021	0.012	0.041	0.017	0.058	0.005	0.125	0.226	98.226	0.000	0.139
1-JGHX-20AC	480	1.472	0.022	0.014	0.041	0.018	0.061	0.005	0.125	0.100	98.100	0.000	0.144
1-JGHX-21A	482	1.277	0.018	0.015	0.030	0.018	0.080	0.005	0.125	0.295	98.295	0.000	0.148
1-JGHX-21B	484	1.040	0.011	0.015	0.024	0.012	0.032	0.000	0.104	0.171	98.171	0.000	0.091
1-JGHX-21C	485	0.819	0.000	0.015	0.020	0.008	0.021	0.000	0.092	0.970	98.970	0.000	0.056
1-JGHX-21D	491	0.289	0.000	0.000	0.020	0.004	0.000	0.000	0.092	99.523	0.000	0.072	
1-JGHX-21E	493	0.358	0.000	0.005	0.020	0.000	0.021	0.000	0.091	99.489	0.000	0.037	
1-JGHX-21F	487	1.898	0.048	0.000	0.032	0.038	0.034	0.011	0.098	97.887	0.000	0.188	
1-JGHX-21G	518	0.818	0.030	0.000	0.034	0.048	0.038	0.031	0.010	98.862	0.000	0.328	
1-JGHX-21H	517	0.588	0.028	0.013	0.032	0.033	0.034	0.022	0.008	98.989	0.000	0.288	
1-JGHX-21I	211	1.342	0.031	0.028	0.032	0.029	0.035	0.018	0.100	98.228	0.000	0.159	
1-JGHX-21J	530	2.407	0.033	0.000	0.041	0.025	0.053	0.010	0.114	97.152	0.000	0.188	
1-JGHX-21K	534	1.589	0.022	0.000	0.041	0.017	0.054	0.005	0.120	98.038	0.000	0.135	
1-JGHX-21L	540	1.328	0.070	0.000	0.000	0.050	0.000	0.000	0.118	98.352	0.000	0.083	
1-JGHX-21M	548	1.245	0.073	0.000	0.000	0.058	0.000	0.000	0.118	98.448	0.000	0.081	
1-JGHX-21N	548	1.340	0.074	0.000	0.000	0.058	0.000	0.000	0.120	98.350	0.000	0.058	
1-JGHX-21O	552	1.560	0.071	0.000	0.000	0.054	0.000	0.000	0.120	98.134	0.000	0.082	
1-JGHX-21P	553	1.747	0.025	0.000	0.050	0.000	0.072	0.000	0.000	97.802	0.000	0.205	
1-JGHX-21Q	558	1.304	0.058	0.000	0.000	0.051	0.000	0.000	0.117	98.408	0.000	0.088	
1-JGHX-21R	580	1.843	0.058	0.000	0.000	0.054	0.000	0.000	0.117	98.147	0.000	0.080	
1-JGHX-21S	586	1.182	0.048	0.000	0.000	0.037	0.000	0.000	0.083	98.528	0.000	0.128	
1-JGHX-21T	575	1.423	0.081	0.000	0.000	0.048	0.000	0.000	0.118	98.208	0.083	0.081	
1-JGHX-21U	577	1.818	0.088	0.000	0.000	0.080	0.000	0.000	0.112	97.849	0.031	0.088	
1-JGHX-21V	581	1.832	0.082	0.000	0.000	0.044	0.000	0.000	0.110	97.884	0.000	0.088	
1-JGHX-21W	601	1.759	0.080	0.000	0.000	0.043	0.000	0.000	0.110	97.957	0.000	0.071	
1-JGHX-21X	603	1.875	0.058	0.000	0.000	0.044	0.000	0.000	0.111	97.838	0.000	0.078	
1-JGHX-21Y	603	1.875	0.058	0.000	0.000	0.044	0.000	0.000	0.111	97.838	0.000	0.078	
1-JGHX-21Y	607	1.713	0.000	0.000	0.000	0.018	0.000	0.000	0.101	98.187	0.000	0.000	
1-JGHX-23A	815	1.919	0.000	0.000	0.000	0.000	0.000	0.000	0.075	98.005	0.000	0.000	
1-JGHX-23B	817	1.787	0.000	0.000	0.000	0.000	0.000	0.000	0.075	98.158	0.000	0.000	
1-JGHX-23C	821	1.548	0.000	0.000	0.014	0.000	0.000	0.000	0.075	98.385	0.000	0.000	
1-JGHX-23D	828	1.305	0.000	0.000	0.018	0.000	0.000	0.000	0.088	98.591	0.000	0.000	
1-JGHX-23E	831	1.848	0.000	0.000	0.021	0.000	0.000	0.000	0.093	98.038	0.000	0.000	
1-JGHX-23F	835	1.483	0.000	0.000	0.019	0.000	0.000	0.000	0.088	98.430	0.000	0.000	
1-JGHX-23G	841	0.250	0.000	0.000	0.000	0.000	0.000	0.000	0.072	99.579	0.000	0.000	
1-JGHX-23H	842	0.085	0.000	0.000	0.000	0.000	0.000	0.000	0.037	99.897	0.000	0.000	
1-JGHX-23I	848	0.077	0.000	0.000	0.000	0.000	0.000	0.000	0.080	99.844	0.000	0.000	
1-JGHX-23J	853	0.081	0.000	0.000	0.014	0.000	0.000	0.000	0.081	99.824	0.000	0.000	
1-JGHX-23K	854	0.170	0.000	0.000	0.015	0.000	0.000	0.000	0.083	99.732	0.000	0.000	
1-JGHX-23L	881	0.118	0.000	0.000	0.018	0.000	0.000	0.000	0.098	99.770	0.000	0.000	
1-JGHX-23M	878	0.048	0.000	0.000	0.017	0.000	0.000	0.000	0.088	99.849	0.000	0.000	

Table 12. Aqueous Layer Analyses, Weight Percent

SAMPLE REF.	CO RUN	MEOH	ETOH	I-PROH	T-BUOH	N-PROH	S-BUOH	I-BUOH	N-BUOH	DODECANE	GLYME	MISC
1-JGHX-18B	0	0.000	0.000	0.000	0.000	0.000	0.000	0.000	0.000	0.000	0.000	0.000
1-JGHX-18C	0	0.000	0.000	0.000	0.000	0.000	0.000	0.000	0.000	0.000	0.000	0.000
1-JGHX-18D	0	33.979	7.025	0.197	0.000	0.000	0.000	0.000	0.074	0.187	17.643	0.000
1-JGHX-18E	0	94.488	0.000	0.030	0.000	0.000	0.000	0.000	0.084	0.279	4.488	0.000
1-JGHX-18F	298	4.848	0.008	0.020	0.000	0.004	0.000	0.000	0.084	95.050	0.000	0.000
1-JGHX-18G	348	91.812	1.261	0.100	0.000	0.518	0.117	0.009	0.083	3.798	2.028	0.578
1-JGHX-18H	349	82.428	0.841	0.044	0.000	0.482	0.098	0.022	0.088	4.084	31.240	0.738
1-JGHX-18I	0	0.000	0.000	0.000	0.000	0.000	0.000	0.000	0.000	0.000	0.000	0.000
1-JGHX-18J	0	0.000	0.000	0.000	0.000	0.000	0.000	0.000	0.000	0.000	0.000	0.000
1-JGHX-18K	0	0.000	0.000	0.000	0.000	0.000	0.000	0.000	0.000	0.000	0.000	0.000
1-JGHX-18L	0	0.000	0.000	0.000	0.000	0.000	0.000	0.000	0.000	0.000	0.000	0.000
1-JGHX-20A	0	0.000	0.000	0.000	0.000	0.000	0.000	0.000	0.000	0.000	0.000	0.000
1-JGHX-20B	0	0.000	0.000	0.000	0.000	0.000	0.000	0.000	0.000	0.000	0.000	0.000
1-JGHX-20C	0	0.000	0.000	0.000	0.000	0.000	0.000	0.000	0.000	0.000	0.000	0.000
1-JGHX-20D	0	0.000	0.000	0.000	0.000	0.000	0.000	0.000	0.000	0.000	0.000	0.000
1-JGHX-20E	0	0.000	0.000	0.000	0.000	0.000	0.000	0.000	0.000	0.000	0.000	0.000
1-JGHX-20F	0	0.000	0.000	0.000	0.000	0.000	0.000	0.000	0.000	0.000	0.000	0.000
1-JGHX-20G	0	0.000	0.000	0.000	0.000	0.000	0.000	0.000	0.000	0.000	0.000	0.000
1-JGHX-20H	0	0.000	0.000	0.000	0.000	0.000	0.000	0.000	0.000	0.000	0.000	0.000
1-JGHX-20I	0	0.000	0.000	0.000	0.000	0.000	0.000	0.000	0.000	0.000	0.000	0.000
1-JGHX-20J	0	0.000	0.000	0.000	0.000	0.000	0.000	0.000	0.000	0.000	0.000	0.000
1-JGHX-20K	0	0.000	0.000	0.000	0.000	0.000	0.000	0.000	0.000	0.000	0.000	0.000
1-JGHX-20L	0	0.000	0.000	0.000	0.000	0.000	0.000	0.000	0.000	0.000	0.000	0.000
1-JGHX-20M	0	0.000	0.000	0.000	0.000	0.000	0.000	0.000	0.000	0.000	0.000	0.000
1-JGHX-20N	0	0.000	0.000	0.000	0.000	0.000	0.000	0.000	0.000	0.000	0.000	0.000
1-JGHX-20O	0	0.000	0.000	0.000	0.000	0.000	0.000	0.000	0.000	0.000	0.000	0.000
1-JGHX-20P	0	0.000	0.000	0.000	0.000	0.000	0.000	0.000	0.000	0.000	0.000	0.000
1-JGHX-20Q	0	0.000	0.000	0.000	0.000	0.000	0.000	0.000	0.000	0.000	0.000	0.000
1-JGHX-20R	0	0.000	0.000	0.000	0.000	0.000	0.000	0.000	0.000	0.000	0.000	0.000
1-JGHX-20S	0	0.000	0.000	0.000	0.000	0.000	0.000	0.000	0.000	0.000	0.000	0.000
1-JGHX-20T	0	0.000	0.000	0.000	0.000	0.000	0.000	0.000	0.000	0.000	0.000	0.000
1-JGHX-20U	0	0.000	0.000	0.000	0.000	0.000	0.000	0.000	0.000	0.000	0.000	0.000
1-JGHX-20V	480	93.339	0.000	0.028	0.029	0.310	0.071	0.047	0.074	3.719	0.999	0.784
1-JGHX-20W	0	0.000	0.000	0.000	0.000	0.000	0.000	0.000	0.000	0.000	0.000	0.000
1-JGHX-20X	483	88.898	0.000	1.882	0.048	0.952	0.173	0.528	0.138	5.123	0.000	2.267
1-JGHX-20y	0	0.000	0.000	0.000	0.000	0.000	0.000	0.000	0.000	0.000	0.000	0.000
1-JGHX-20Z	0	0.000	0.000	0.000	0.000	0.000	0.000	0.000	0.000	0.000	0.000	0.000
1-JGHX-20AA475	0	88.431	1.289	0.089	0.088	0.582	0.127	0.264	0.407	8.083	0.000	8.838
1-JGHX-20AB477	0	92.048	0.288	0.000	0.000	0.198	0.070	0.098	0.330	6.017	0.000	1.014
1-JGHX-20AC479	0	92.233	1.243	0.105	0.000	0.474	0.111	0.118	0.329	4.728	0.000	0.868
1-JGHX-21A	481	92.227	1.102	0.040	0.000	0.482	0.116	0.119	0.343	4.894	0.000	0.878
1-JGHX-21B	483	86.404	0.878	0.040	0.000	0.378	0.078	0.078	0.089	7.854	0.488	1.055
1-JGHX-21C	0	0.000	0.000	0.000	0.000	0.000	0.000	0.000	0.000	0.000	0.000	0.000
1-JGHX-21D	492	83.997	0.748	0.280	0.180	0.180	0.048	0.033	0.320	11.868	2.028	0.880
1-JGHX-21E	494	92.181	0.738	0.038	0.000	0.297	0.083	0.043	0.245	4.080	0.844	0.497
1-JGHX-21F	499	88.871	1.002	0.080	0.000	0.857	0.186	0.233	0.129	5.882	0.487	1.482
1-JGHX-21G	0	0.000	0.000	0.000	0.000	0.000	0.000	0.000	0.000	0.000	0.000	0.000
1-JGHX-21H	0	0.000	0.000	0.000	0.000	0.000	0.000	0.000	0.000	0.000	0.000	0.000
1-JGHX-21I	0	0.000	0.000	0.000	0.000	0.000	0.000	0.000	0.000	0.000	0.000	0.000
1-JGHX-21J	0	0.000	0.000	0.000	0.000	0.000	0.000	0.000	0.000	0.000	0.000	0.000
1-JGHX-21K	538	92.182	1.128	0.044	0.000	0.500	0.088	0.134	0.052	0.000	0.000	5.872
1-JGHX-21L	539	86.948	1.005	0.045	0.000	0.428	0.078	0.107	0.311	0.000	10.510	0.571
1-JGHX-21M	547	92.177	1.072	0.000	0.000	0.451	0.088	0.113	0.047	0.000	0.113	5.941
1-JGHX-21N	549	93.739	1.052	0.049	0.000	0.430	0.081	0.105	0.043	3.703	0.097	0.703
1-JGHX-21O	0	0.000	0.000	0.000	0.000	0.000	0.000	0.000	0.000	0.000	0.000	0.000
1-JGHX-21P	554	93.158	1.119	0.081	0.000	0.459	0.088	0.109	0.050	4.148	0.041	0.784
1-JGHX-21Q	0	0.000	0.000	0.000	0.000	0.000	0.000	0.000	0.000	0.000	0.000	0.000
1-JGHX-21R	0	0.000	0.000	0.000	0.000	0.000	0.000	0.000	0.000	0.000	0.000	0.000
1-JGHX-21S	585	92.322	0.572	0.183	0.000	0.140	0.041	0.034	0.079	3.113	2.838	0.678
1-JGHX-21T	578	91.980	0.620	0.298	0.000	0.108	0.083	0.087	0.182	3.742	2.858	0.317
1-JGHX-21U	578	92.873	0.532	0.000	0.104	0.197	0.080	0.056	0.135	5.127	0.744	0.174
1-JGHX-21V	582	93.388	0.498	0.088	0.000	0.187	0.050	0.047	0.128	5.220	0.288	0.189
1-JGHX-21W	602	93.358	0.451	0.000	0.042	0.171	0.039	0.038	0.115	5.494	0.134	0.180
1-JGHX-21X	604	93.889	0.000	0.370	0.045	0.180	0.037	0.034	0.109	5.489	0.085	0.133
1-JGHX-21X	604	93.559	0.000	0.370	0.045	0.180	0.037	0.034	0.109	5.489	0.085	0.133
1-JGHX-21Y	608	93.880	0.288	0.088	0.000	0.088	0.000	0.000	0.088	5.580	0.000	0.658
1-JGHX-23A	618	94.139	0.048	0.077	0.000	0.038	0.000	0.000	0.040	5.385	0.247	0.028
1-JGHX-23B	618	94.242	0.038	0.000	0.000	0.087	0.000	0.000	0.038	5.438	0.170	0.024
1-JGHX-23C	622	90.809	0.190	0.072	0.000	0.102	0.000	0.000	0.000	0.988	0.120	7.713
1-JGHX-23D	630	92.188	0.257	0.000	0.083	0.128	0.000	0.000	0.117	5.182	0.292	1.804
1-JGHX-23E	632	93.947	0.000	0.229	0.084	0.128	0.000	0.000	0.117	5.137	0.218	0.188
1-JGHX-23F	636	93.757	0.353	0.000	0.087	0.124	0.000	0.000	0.115	5.208	0.185	0.188
1-JGHX-23G	0	0.000	0.000	0.000	0.000	0.000	0.000	0.000	0.000	0.000	0.000	0.000
1-JGHX-23H	0	0.000	0.000	0.000	0.000	0.000	0.000	0.000	0.000	0.000	0.000	0.000
1-JGHX-23I	0	0.000	0.000	0.000	0.000	0.000	0.000	0.000	0.000	0.000	0.000	0.000
1-JGHX-23J	0	0.000	0.000	0.000	0.000	0.000	0.000	0.000	0.000	0.000	0.000	0.000
1-JGHX-23K	0	0.000	0.000	0.000	0.000	0.000	0.000	0.000	0.000	0.000	0.000	0.000
1-JGHX-23L	0	0.000	0.000	0.000	0.000	0.000	0.000	0.000	0.000	0.000	0.000	0.000
1-JGHX-23M	0	0.000	0.000	0.000	0.000	0.000	0.000	0.000	0.000	0.000	0.000	0.000

Table 13. Reaction Conditions.

RUN ID	DATE	TIME	H ₂ FEED scfm	CO FEED scfm	N ₂ FEED scfm	OFF GAS scfm	OFF GAS TEMP °C	LIQUID FEED g/hr	HX TEMP °C	HX PRES psig	DAWG PRES mm Hg	OV ₂ WT g	AO ₂ WT g	DELTA TIME hr	AGITATOR RPM	mech FEED Q/HR	TOTAL TIME hr
I-JCHX-18B	2/13/90	8:05 AM	202	0	0	164.3	23	22.50	240	762	740.0	468.9	0.0	16.6	1350		23
I-JCHX-18C	2/13/90	9:00 AM	202	0	0	164.3	23	22.50	240	753	740.0	34.9	0.1	0.9	1350		24
I-JCHX-18D	2/13/90	11:00 AM	302	151	0	357.7	23	22.50	240	751	740.0	59.4	0.4	2.0	1350		26
I-JCHX-18E	2/13/90	1:00 PM	302	151	0	357.7	23	22.50	240	750	740.0	66.0	2.0	2.0	1350		28
I-JCHX-18F	2/13/90	3:00 PM	302	151	0	333.8	23	22.50	240	750	740.0	66.7	1.5	2.0	1373		30
I-JCHX-18G	2/14/90	12:00 AM	302	151	0	357.7	23	22.50	240	750	740.0	266.5	0.5	0.0	1373		30
I-JCHX-18H	2/14/90	8:00 AM	302	151	0	357.7	23	22.50	240	750	740.0	152.5	0.5	6.0	1373		47
I-JCHX-18I	2/14/90	1:00 PM	302	151	0	357.8	23	22.50	240	751	740.0	94.4	0.0	5.0	1373		52
I-JCHX-18J	2/14/90	3:00 PM	302	151	0	357.7	23	22.50	240	750	740.0	39.2	0.0	2.0	1373		54
I-JCHX-18K	2/15/90	12:00 AM	302	151	0	357.8	23	22.50	240	751	740.0	186.7	0.0	9.0	1373		63
I-JCHX-18L	2/15/90	8:30 AM	302	151	0	357.8	23	22.50	240	751	740.0	181.8	0.0	8.5	1373		71
I-JCHX-20A	2/15/90	11:00 AM	302	150	0	360.0	23	22.50	240	751	740.0	54.5	0.0	2.5	1373		74
I-JCHX-20B	2/15/90	3:00 PM	302	149	0	360.0	23	11.25	240	751	740.0	81.1	0.0	4.0	1373		78
I-JCHX-20C	2/16/90	12:00 AM	302	151	0	366.1	23	11.25	240	749	760.0	81.1	0.0	9.0	1373		87
I-JCHX-20D	2/16/90	7:00 AM	302	151	0	364.9	22	11.25	240	749	754.8	77.0	0.0	7.0	1373		94
I-JCHX-20E	2/16/90	11:00 AM	302	150	0	351.7	23	11.25	240	749	740.0	40.3	0.0	4.0	1373		96
I-JCHX-20F	2/16/90	3:30 PM	302	151	0	366.4	23	11.25	240	751	740.0	46.4	0.0	4.5	1373		102
I-JCHX-20G	2/16/90	11:59 AM	302	151	0	365.7	23	11.25	240	751	740.0	90.0	0.0	6.5	1373		111
I-JCHX-20H	2/19/90	7:30 AM	302	151	0	365.7	23	11.25	240	751	740.0	593.6	0.0	55.5	1373		166
I-JCHX-20I	2/19/90	3:00 PM	302	151	0	405.4	23	11.25	239	750	740.0	83.5	0.0	7.5	1373		174
I-JCHX-20J	2/19/90	11:00 PM	302	151	0	411.8	23	11.25	239	750	740.0	81.0	0.0	6.0	1373		182
I-JCHX-20K	2/20/90	7:00 AM	302	151	0	420.2	23	11.25	240	750	755.0	84.4	0.0	6.0	1373		190
I-JCHX-20L	2/20/90	3:00 PM	302	151	0	366.3	23	11.25	240	750	755.0	94.3	0.0	6.0	1373		198
I-JCHX-20M	2/20/90	11:00 PM	323	131	0	398.8	23	11.25	240	750	758.0	82.8	0.0	8.0	1373		206
I-JCHX-20N	2/21/90	7:00 AM	323	131	0	391.4	23	11.25	220	552	742.0	83.3	0.0	8.0	1373		214
I-JCHX-20O	2/21/90	3:00 PM	323	131	0	388.1	23	11.25	220	552	750.0	91.9	0.0	8.0	1373		222
I-JCHX-20P	2/22/90	7:00 AM	323	131	0	395.2	23	11.25	220	552	740.0	176.6	0.0	16.0	1373		238
I-JCHX-20Q	2/22/90	3:00 PM	272	181	0	340.1	23	11.25	220	950	735.0	143.0	0.0	8.0	1300		246
I-JCHX-20R	2/22/90	11:00 PM	272	181	0	394.6	23	11.25	220	950	735.0	119.6	0.0	8.0	1300		254
I-JCHX-20S	2/23/90	7:00 AM	272	181	0	393.5	23	11.25	220	950	733.0	210.2	0.0	8.0	1300		262
I-JCHX-20T	2/23/90	3:00 PM	272	181	0	397.0	23	11.25	220	950	735.0	66.3	0.0	6.0	1300		270
I-JCHX-20U	2/24/90	11:00 PM	302	151	0	417.1	23	11.25	240	750	735.0	348.8	0.5	32.0	1300		302
I-JCHX-20V	2/25/90	7:30 AM	302	151	0	433.9	22	11.25	240	750	782.0	359.1	1.0	32.5	1300		334
I-JCHX-20W	2/25/90	3:00 PM	272	181	0	404.9	22	2.00	260	550	759.0	18.9	0.0	7.5	1300		342
I-JCHX-20X	2/26/90	11:00 PM	272	181	0	395.6	22	6.00	260	550	750.0	47.6	1.0	8.0	1300		350
I-JCHX-20Y	2/27/90	7:30 AM	272	181	0	392.5	22	11.25	260	550	753.0	92.5	0.0	8.5	1319		358
I-JCHX-20Z	2/27/90	3:00 PM	272	181	0	392.5	22	11.25	260	550	753.0	80.2	0.0	7.5	1319		366
I-JCHX-20AA	2/27/90	11:00 PM	323	131	0	398.3	22	11.25	260	950	754.0	83.3	2.8	8.0	1319		374
I-JCHX-20AB	2/28/90	8:15 AM	323	131	0	396.1	22	11.25	260	950	754.0	101.7	6.8	9.3	1319		383
I-JCHX-20AC	2/28/90	3:00 PM	323	131	0	341.7	22	11.25	260	950	753.5	74.8	4.2	6.8	1319		390
I-JCHX-21A	2/28/90	11:00 PM	323	131	0	366.8	22	11.25	260	950	754.0	93.1	3.2	8.0	1319		398
I-JCHX-21B	3/1/90	8:20 AM	302	151	0	387.2	22	11.25	240	750	754.8	106.1	0.8	9.3	1319		407
I-JCHX-21C	3/1/90	3:00 PM	302	151	0	389.5	22	11.25	240	750	754.8	72.4	0.0	6.7	1319		414
I-JCHX-21D	3/1/90	11:00 PM	302	151	0	377.6	22	11.25	240	750	754.8	86.8	0.1	6.0	1319		422
I-JCHX-21E	3/2/90	7:00 AM	302	151	0	373.4	22	11.25	240	750	746.0	91.1	0.7	6.0	1319		430
I-JCHX-21F	3/2/90	3:00 PM	152	202	0	342.8	22	11.25	260	950	748.0	77.2	0.0	8.0	1373		438
I-JCHX-21G	3/3/90	11:00 PM	152	202	0	292.8	22	11.25	260	952	746.0	350.7	0.0	32.0	1323		470
I-JCHX-21H	3/5/90	7:15 AM	152	202	0	294.0	22	11.25	260	952	740.0	352.9	0.0	32.3	1323		502
I-JCHX-21I	3/5/90	3:00 PM	227	76	0	232.4	22	11.25	259	948	748.0	85.8	9.0	7.8	1500		510
I-JCHX-21J	3/5/90	11:00 PM	227	76	0	225.8	22	11.25	259	948	748.0	89.2	0.0	8.0	1500		518
I-JCHX-21K	3/6/90	7:30 AM	227	76	0	226.6	22	11.25	259	946	750.5	93.4	1.3	8.5	1500		526
I-JCHX-21L	3/6/90	3:00 PM	227	76	0	227.3	22	11.25	259	948	751.5	82.5	1.8	7.5	1375		534
I-JCHX-21M	3/6/90	11:00 PM	227	76	0	227.3	22	11.25	259	948	751.5	87.5	1.5	8.0	1375		542
I-JCHX-21N	3/7/90	7:00 AM	227	76	0	228.8	22	11.25	260	948	756.0	88.2	2.0	8.0	1375		550
I-JCHX-21O	3/7/90	11:00 AM	227	76	0	226.4	23	11.25	260	949	756.5	45.0	0.0	4.0	1390		554
I-JCHX-21P	3/7/90	3:00 PM	668	335	0	862.4	21	11.25	260	948	755.0	50.7	3.0	4.0	1390		558
I-JCHX-21Q	3/7/90	11:00 PM	668	335	0	910.7	22	11.25	260	948	755.0	87.8	0.0	8.0	1390		566
I-JCHX-21R	3/8/90	7:00 AM	668	335	0	909.5	22	11.25	260	948	754.0	88.9	0.0	8.0	1390		574
I-JCHX-21S	3/8/90	3:00 PM	189	84	0	178.1	23	11.25	260	952	751.5	88.1	2.0	8.0	1390	1.33	582
I-JCHX-21T	3/8/90	11:00 PM	189	84	0	217.0	22	11.25	260	952	748.0	87.6	11.8	8.0	1390	3.31	590
I-JCHX-21U	3/9/90	7:00 AM	189	84	0	217.0	22	11.25	260	951	748.0	89.6	14.6	8.0	1390	3.31	598
I-JCHX-21V	3/9/90	3:00 PM	189	84	0	219.1	23	11.25	260	952	747.0	88.9	15.6	8.0	1390	3.50	606
I-JCHX-21W	3/10/90	11:00 PM	189	84	0	232.7	22	11.25	260	952	747.0	350.4	64.3	32.0	1390	3.59	638
I-JCHX-21X	3/12/90	7:00 AM	189	84	0	232.3	23	11.25	261	952	748.0	352.6	65.4	32.0	1390	3.59	670
I-JCHX-21Y	3/12/90	7:00 AM	189	84	0	232.3	23	11.25	261	952	748.0	352.6	65.4	32.0	1390	3.59	670
I-JCHX-21Z	3/12/90	3:00 PM	668	335	0	869.3	24	11.25	220	946	748.0	99.8	18.0	8.0	1390	3.50	678
I-JCHX-23A	3/12/90	11:00 PM	668	335	0	994.2	22	11.25	219	948	746.0	80.1	5.0	8.0	1390	3.46	686
I-JCHX-23B	3/13/90	7:00 AM	668	335	0	983.5	23	11.25	219	948	748.0	88.3	8.1	8.0	1390	3.46	694
I-JCHX-23C	3/13/90	3:00 PM	335	169	0	518.3	24	11.25	240	951	748.0	82.4	6.7	8.0	1390	1.83	702
I-JCHX-23D	3/13/90	11:00 PM	335	169	0	474.7	24	11.25	240	954	746.0	87.5	2.3	8.0	1390	1.80	710
I-JCHX-23E	3/14/90	7:00 AM	335	169	0	473.5	24	11.25	240	948	744.0	89.1	2.6	8.0	1390	1.30	718
I-JCHX-23F	3/14/90	3:00 PM	335	169	0	481.1	24	11.25	239	951	742.0	87.3	2.5	8.0	1390	1.63	726
I-JCHX-23G	3/14/90	11:00 PM	188	84	0	235.4	24	11.25	220	951	742.0	84.7	0.0	8.0	1390	0.00	734
I-JCHX-23H	3/15/90	7:00 AM	188	84	0	235.8	24	11.25	220	948	743.0	85.6	0.0	8.0	1390	0.00	742
I-JCHX-23I	3/15/90	3:00 PM	189	84	0	234.0	25	11.25	220	949	743.0	85.3</					

Table 14. Methanol Productivities and Material Balances.

SAMPLE REF	NET SOLVENT GRAMS	MEOH LIQUID G/HR	MEOH GAS G/HR	MEOH TOTAL G/HR	TOTAL HOURS	G FED M/HR	G ROVD GAS M/HR	G ROVD LIQUID M/HR	CO ROVD TOTAL M/HR	ERROR %	SOLVENT IN RX G	TOTAL FED G	conversion o-based	efficiency o-based
I-JGHX-18B	95.0	0.014	0.000	0.01	23.1	0.0000	0.0018	0.0022	0.0040		710	710		
I-JGHX-18C	14.2	0.010	0.000	0.01	24.0	0.0000	0.0009	0.0017	0.0026		616	1003		
I-JGHX-18D	14.3	0.079	4.398	4.47	26.0	0.4048	0.3685	0.0047	0.3832	12.7	586	1149	34.6	85.6
I-JGHX-18E	20.6	1.123	2.132	3.25	23.0	0.4048	0.3423	0.0367	0.3790	-6.3	566	1194	28.1	92.0
I-JGHX-18F	24.4	0.362	2.078	2.44	30.0	0.4045	0.3310	0.0131	0.3441	14.9	541	1239	18.8	83.8
I-JGHX-18G	62.5	0.406	2.184	2.57	39.0	0.4045	0.3648	0.0146	0.3794	-6.2	479	1441	19.8	92.0
I-JGHX-18H	30.4	0.214	1.898	2.11	47.0	0.4045	0.3584	0.0082	0.3666	-9.4	509	1621	16.3	80.4
I-JGHX-18I	17.2	0.088	1.648	1.73	52.0	0.4045	0.3548	0.0033	0.3579	-11.5	527	1734	13.4	87.2
I-JGHX-18J	6.0	0.054	1.648	1.70	54.0	0.4045	0.3646	0.0030	0.3576	-11.6	533	1779	13.1	86.9
I-JGHX-18K	16.3	0.044	1.251	1.30	63.0	0.4045	0.3459	0.0019	0.3478	-14.0	549	1981	10.0	84.7
I-JGHX-18L	10.2	0.045	1.350	1.39	71.5	0.4045	0.3586	0.0019	0.3605	-10.9	559	2172	10.8	88.0
I-JGHX-20A	2.1	0.049	1.192	1.24	74.0	0.4018	0.3503	0.0022	0.3525	-12.3	561	2229	9.7	86.4
I-JGHX-20B	35.0	0.037	1.319	1.36	78.0	0.3991	0.3522	0.0017	0.3539	-11.3	525	2274	10.8	87.3
I-JGHX-20C	20.5	0.036	1.312	1.35	87.0	0.4045	0.3672	0.0016	0.3687	-11.3	546	2376	10.4	87.7
I-JGHX-20D	2.9	0.140	1.974	2.11	94.0	0.4045	0.3782	0.0056	0.3818	-6.6	540	2454	16.3	90.2
I-JGHX-20E	8.3	0.094	1.988	2.08	98.0	0.4018	0.3588	0.0044	0.3630	-9.8	554	2499	16.2	88.7
I-JGHX-20F	4.7	0.099	1.978	2.07	102.5	0.4045	0.3704	0.0035	0.3740	-7.5	559	2549	16.0	90.7
I-JGHX-20G	6.0	0.030	2.027	2.06	111.0	0.4045	0.3884	0.0014	0.3878	-4.1	565	2645	15.9	94.0
I-JGHX-20H	33.5	0.031	1.602	1.63	166.5	0.4045	0.3827	0.0019	0.3846	-4.9	598	3289	12.6	93.5
I-JGHX-20I	1.2	0.038	1.648	1.69	174.0	0.4048	0.4001	0.0018	0.4017	-0.7	599	3354	13.0	97.8
I-JGHX-20J	9.5	0.049	1.783	1.83	182.0	0.4045	0.4007	0.0020	0.4108	1.6	609	3444	14.1	100.1
I-JGHX-20K	6.4	0.077	1.660	1.74	190.0	0.4045	0.4152	0.0036	0.4190	3.6	615	3534	13.4	101.4
I-JGHX-20L	3.7	0.039	1.550	1.59	198.0	0.4045	0.3937	0.0029	0.3966	-1.0	612	3624	12.3	90.2
I-JGHX-20M	7.5	0.015	0.971	0.99	206.0	0.3509	0.2588	0.0016	0.2604	-25.6	619	3714	8.8	72.6
I-JGHX-20N	6.9	0.010	0.925	0.93	214.0	0.3509	0.2393	0.0012	0.2405	-31.5	626	3804	8.3	67.0
I-JGHX-20O	-1.7	0.008	0.894	0.90	222.0	0.3509	0.2020	0.0012	0.2032	13.6	624	3894	6.0	85.4
I-JGHX-20P	3.6	0.007	0.842	0.85	238.0	0.3509	0.2267	0.0010	0.2278	-6.6	628	4074	7.6	92.0
I-JGHX-20Q	52.7	0.025	1.244	1.27	246.0	0.4848	0.4081	0.0017	0.4098	15.5	675	4164	8.2	83.9
I-JGHX-20R	29.3	0.020	1.471	1.49	254.0	0.4848	0.4667	0.0015	0.4682	-3.4	548	4254	9.6	95.8
I-JGHX-20S	119.7	0.031	1.042	1.07	262.0	0.4848	0.4542	0.0023	0.4565	5.6	428	4344	6.9	93.2
I-JGHX-20T	4.0	0.020	1.216	1.24	270.0	0.4848	0.4650	0.0013	0.4663	-3.6	430	4434	6.0	95.4
I-JGHX-20U	16.1	0.069	1.728	1.80	302.0	0.4045	0.4188	0.0034	0.4222	4.4	446	4794	13.9	102.5
I-JGHX-20V	10.0	0.114	1.806	1.92	334.5	0.4045	0.4339	0.0049	0.4388	8.5	456	5159	14.8	106.6
I-JGHX-20W	-3.6	0.032	1.316	1.35	342.0	0.4848	0.4650	0.0015	0.4668	-3.8	453	5174	8.7	91.7
I-JGHX-20X	17.4	0.205	1.118	1.32	350.0	0.4848	0.4842	0.0090	0.4712	2.8	470	5238	8.5	94.7
I-JGHX-20Y	3.7	0.029	1.273	1.30	358.5	0.4848	0.4618	0.0033	0.4651	-4.1	474	5334	6.4	93.5
I-JGHX-20Z	4.8	0.038	1.443	1.48	368.0	0.4848	0.4645	0.0036	0.4681	-3.5	479	5418	9.8	94.0
I-JGHX-20AA	8.0	0.460	1.678	2.14	374.0	0.3509	0.2810	0.0172	0.2982	-15.0	487	5508	19.0	80.9
I-JGHX-20AB	3.8	0.806	1.689	2.50	383.3	0.3509	0.2677	0.0284	0.2961	-15.6	491	5612	22.2	80.4
I-JGHX-20AC	2.4	0.737	1.833	2.57	390.0	0.3509	0.2917	0.0285	0.3182	9.3	493	5688	22.0	85.4
I-JGHX-21A	-1.0	0.760	2.173	2.93	398.0	0.3509	0.3350	0.0274	0.3624	3.3	491	5778	26.1	97.4
I-JGHX-21B	0.7	0.195	1.483	1.68	407.3	0.4045	0.3788	0.0080	0.3868	-4.4	491	5881	12.8	93.6
I-JGHX-21C	3.3	0.089	1.382	1.47	414.0	0.4045	0.3833	0.0040	0.3874	4.2	495	5958	11.4	94.3
I-JGHX-21D	3.6	0.042	1.347	1.39	422.0	0.4045	0.3718	0.0024	0.3740	-7.5	498	6048	10.7	90.7
I-JGHX-21E	0.7	0.121	1.332	1.45	430.0	0.4045	0.3873	0.0049	0.3723	-8.0	498	6138	11.2	90.2
I-JGHX-21F	14.6	0.183	1.887	2.07	438.0	0.5411	0.5704	0.0079	0.5782	6.9	512	6220	11.9	103.4
I-JGHX-21G	14.0	0.069	1.931	1.82	470.0	0.5411	0.5207	0.0059	0.5266	-2.7	528	6588	9.4	94.3
I-JGHX-21H	13.4	0.062	1.480	1.54	502.2	0.5411	0.5182	0.0045	0.5220	-3.4	540	6951	8.9	94.0
I-JGHX-21I	2.9	0.149	1.258	1.40	510.0	0.2036	0.1980	0.0072	0.2052	0.8	543	7038	21.6	98.9
I-JGHX-21J	3.3	0.268	1.343	1.61	510.0	0.2036	0.1820	0.0110	0.1930	-5.2	546	7128	24.7	87.6
I-JGHX-21K	4.1	0.313	1.183	1.50	526.5	0.2036	0.1659	0.0128	0.1787	12.2	550	7224	23.0	80.2
I-JGHX-21L	3.2	0.355	1.245	1.60	534.0	0.2036	0.1681	0.0132	0.1813	10.9	553	7308	24.5	82.2
I-JGHX-21M	3.9	0.309	1.292	1.57	542.0	0.2036	0.1658	0.0122	0.1780	-12.8	557	7399	24.1	80.3
I-JGHX-21N	3.2	0.382	1.457	1.84	550.0	0.2036	0.1729	0.0140	0.1869	-8.2	560	7488	26.2	84.7
I-JGHX-21O	0.8	0.175	1.194	1.37	554.0	0.2036	0.1410	0.0072	0.1483	27.2	561	7533	21.0	70.6
I-JGHX-21P	4.8	0.920	2.175	3.09	558.0	0.8973	0.8018	0.0321	0.8338	-7.1	568	7578	10.8	90.8
I-JGHX-21Q	3.6	0.143	1.979	2.12	568.0	0.8973	0.6680	0.0061	0.6741	2.6	569	7668	7.4	95.8
I-JGHX-21R	2.7	0.172	2.138	2.31	574.0	0.8973	0.6704	0.0071	0.6776	-2.2	583	7758	8.0	96.1
I-JGHX-21S	5.1	0.358	1.072	0.10	582.0	0.2866	0.1802	0.0131	0.1832	-17.5	586	7848	1.2	49.9
I-JGHX-21T	3.6	1.812	1.600	-0.20	590.0	0.3285	0.2284	0.0500	0.2764	18.2	571	7938	1.9	43.1
I-JGHX-21U	1.6	1.898	1.728	0.31	598.0	0.3285	0.2302	0.0621	0.2924	11.0	573	8028	3.0	52.0
I-JGHX-21V	2.2	2.024	1.720	0.25	606.0	0.3343	0.2336	0.0659	0.2995	-10.4	575	8118	2.3	52.3
I-JGHX-21W	13.2	2.068	1.854	0.33	638.0	0.3371	0.2501	0.0672	0.3173	-5.9	588	8478	3.1	56.8
I-JGHX-21X	11.5	2.119	1.673	0.20	670.0	0.3371	0.2475	0.0687	0.3162	-6.2	600	8838	1.9	56.3
I-JGHX-21Y	11.5	2.119	1.851	0.38	670.0	0.3371	0.2496	0.0687	0.3183	-5.6	611	9198	3.5	57.1
I-JGHX-21Z	-8.8	2.328	2.911	1.74	678.0	1.0088	0.9928	0.0739	1.0665	5.9	602	9288	5.4	94.7
I-JGHX-23A	2.4	0.802	2.718	0.06	686.0	1.0053	0.9549	0.0258	0.9805	-2.5	605	9378	0.2	86.4
I-JGHX-23B	3.0	0.914	2.707	0.18	694.0	1.0053	0.9921	0.0290	0.9911	-1.4	608	9468	0.5	87.4
I-JGHX-23C	8.9	0.239	2.045	0.66	702.0	0.8034	0.5135	0.0683	0.5218	3.7	617	9558	4.1	82.4
I-JGHX-23D	3.6	0.408	1.870	0.48	710.0	0.8089	0.4699	0.0137	0.4837	5.0	620	9648	2.9	83.0
I-JGHX-23E	2.5	0.511	1.768	0.48	718.0	0.8089	0.4648	0.0188	0.4816	5.4	623	9738	2.9	82.3
I-JGHX-23F	3.9	0.453	1.904	0.73	726.0	0.5034	0.4746	0.0149	0.4895	-2.8	627	9828	4.5	85.9
I-JGHX-23G	5.6	0.026	0.628	0.65	734.0	0.2260	0.2273	0.0012	0.2285	1.5	632	9918	9.1	100.2
I-JGHX-23H	4.5	0.007	0.514	0.52	742.0	0.2250	0.2242	0.0004	0.2247	-0.1	637	10008	7.2	98.6
I-JGHX-23I	4.8	0.008	0.483	0.47	750.0	0.2250	0.2248	0.0007	0.2255	0.2	642	10098	6.5	98.9
I-JGHX-23J	5.4	0.009	0.574	0.58	758.0	0.2250	0.2490	0.0008	0.2499	11.0	647	10188	8.1	100.7
I-JGHX-23K	0.9	0.019	0.573	0.59	766.5	0.2250	0.2487	0.0012	0.2499	11.1	648	10284	8.2	100.7
I-JGHX-23L	4.3	0.012	0.705	0.72	774.0	0.4071	0.4137	0.0010	0.4147	1.9	652	10368	5.5	100.5
I-JGHX-23M	13.4	0.005	0.778	0.78	806.0	0.4071	0.4185	0.0008	0.4193	3.0	666	10728	6.0	101.4

Table 15. Calculation of Methanol Productivity and Reactant Partial Pressures.

sample ref	TIME HOURS	TEMP °C	pressure psig	h2 feed scfm	co feed scfm	total flow scfm	off gas scfm	meth feed g/hr	meth prod g/hr	h2 psia	co psia	co2 psia	ch4 psia	total psia	ch4 mg/hr	co2 g/hr	meth g/hr		
1-JGHX-18B	23.1	240	782	202	0	202	184.3	0.00	0	0.6	519.7	0.0	2.8	0.0	304.4	0.0000	0.0180	0.014	
1-JGHX-18C	24.0	240	783	202	0	202	184.3	0.00	0	0.6	519.7	0.0	2.8	0.0	304.4	0.0000	0.0021	0.010	
1-JGHX-18D	28.0	240	781	302	181	2.00	453	357.7	0.00	1	111.3	459.0	164.7	3.6	0.0	523.7	0.0000	0.0202	4.475
1-JGHX-18E	28.0	240	780	302	181	2.00	453	357.7	0.00	13	78.2	447.4	208.1	2.7	0.0	721.6	0.0000	0.0167	3.264
1-JGHX-18F	30.0	240	750	302	181	2.00	453	333.8	0.00	4	64.3	469.4	221.9	2.8	0.0	743.8	0.0000	0.0149	2.440
1-JGHX-18G	39.0	240	760	302	181	2.00	453	357.7	0.00	6	63.2	463.6	229.7	4.2	0.1	745.9	2.2727	0.0237	2.670
1-JGHX-18H	47.0	240	760	302	181	2.00	453	357.7	0.00	2	52.2	471.0	234.3	2.8	0.0	746.5	0.7797	0.0157	2.109
1-JGHX-18I	52.0	240	761	302	181	2.00	453	357.8	0.00	1	43.1	477.8	237.9	3.6	0.0	747.5	0.0000	0.0205	1.733
1-JGHX-18J	54.0	240	760	302	181	2.00	453	357.7	0.00	1	42.2	477.5	237.8	3.6	0.0	746.5	0.7798	0.0205	1.698
1-JGHX-18K	63.0	240	761	302	181	2.00	453	357.8	0.00	1	32.3	484.8	241.1	3.7	0.0	747.2	0.0000	0.0209	1.295
1-JGHX-18L	71.5	240	761	302	181	2.00	453	357.8	0.00	1	34.7	473.8	249.3	3.2	0.0	746.1	0.0000	0.0180	1.395
1-JGHX-20A	74.0	240	761	302	150	2.01	452	360.0	0.00	1	30.7	484.8	244.4	3.9	0.0	749.0	0.0000	0.0218	1.241
1-JGHX-20B	78.0	240	761	302	149	2.03	451	360.0	0.00	0	33.6	483.9	242.7	3.8	0.0	749.3	0.0000	0.0217	1.366
1-JGHX-20C	87.0	240	749	302	151	2.00	453	368.1	0.00	0	32.8	483.4	243.2	2.8	0.0	747.5	0.0000	0.0162	1.350
1-JGHX-20D	94.0	240	749	302	151	2.00	453	364.9	0.00	2	61.3	466.2	232.3	12.0	0.4	747.2	8.7360	0.0691	2.114
1-JGHX-20E	98.0	240	749	302	150	2.01	452	361.7	0.00	1	62.5	470.1	235.8	4.1	0.0	747.5	0.0000	0.0225	2.080
1-JGHX-20F	102.5	240	761	302	151	2.00	453	368.4	0.00	1	60.4	473.3	234.9	5.2	0.0	749.1	0.0000	0.0300	2.075
1-JGHX-20G	111.0	240	761	302	151	2.00	453	365.7	0.00	0	47.5	478.4	234.0	5.2	0.0	750.4	0.0000	0.0312	2.067
1-JGHX-20H	166.5	240	761	302	151	2.00	453	365.7	0.00	0	37.7	478.9	242.4	3.9	0.0	748.2	0.0000	0.0235	1.633
1-JGHX-20I	174.0	239	760	302	11	2.00	453	406.4	0.00	0	37.0	480.7	241.3	3.9	0.0	746.2	0.0000	0.0260	1.685
1-JGHX-20J	182.0	239	760	302	151	2.00	453	411.8	0.00	1	39.8	479.3	240.5	3.8	0.0	746.5	0.0000	0.0247	1.832
1-JGHX-20K	190.0	240	760	302	151	2.00	453	420.2	0.00	1	36.7	478.9	241.2	4.1	0.9	746.3	21.6743	0.0274	1.736
1-JGHX-20L	198.0	240	760	302	151	2.00	453	393.3	0.00	0	36.5	479.8	243.1	4.0	0.0	747.7	0.0000	0.0252	1.589
1-JGHX-20M	206.0	220	652	323	131	2.47	454	398.8	0.00	0	22.0	578.8	160.3	3.2	0.0	749.4	0.0000	0.0200	0.966
1-JGHX-20N	214.0	220	652	323	131	2.47	464	391.4	0.00	0	16.8	435.3	111.3	2.4	0.0	660.1	0.0000	0.0199	0.935
1-JGHX-20O	222.0	220	652	323	131	2.47	464	388.1	0.00	0	15.3	401.8	148.0	1.4	0.0	661.6	0.0000	0.0112	0.902
1-JGHX-20P	236.0	220	652	323	131	2.47	464	393.2	0.00	0	14.2	390.6	158.8	2.2	0.0	551.2	0.0000	0.0189	0.849
1-JGHX-20Q	246.0	220	650	272	181	1.60	453	349.1	0.00	0	40.8	541.8	378.3	2.3	0.0	948.3	0.0000	0.0099	1.239
1-JGHX-20R	264.0	220	650	272	181	1.60	453	394.6	0.00	0	42.4	536.6	381.1	2.8	0.0	946.1	0.0000	0.0138	1.431
1-JGHX-20S	262.0	220	650	272	181	1.60	453	393.5	0.00	0	30.8	547.2	382.5	3.1	0.0	946.7	0.0000	0.0150	1.073
1-JGHX-20T	270.0	220	650	272	181	1.60	453	397.0	0.00	0	36.0	541.0	384.2	3.0	0.0	946.6	0.0000	0.0147	1.236
1-JGHX-20U	302.0	240	760	302	151	2.00	453	417.1	0.00	1	36.3	473.7	244.9	4.3	0.0	745.6	0.0000	0.0281	1.796
1-JGHX-20V	334.5	240	760	302	151	2.00	453	433.9	0.00	1	39.3	475.6	243.4	4.2	0.0	747.7	0.0000	0.0290	1.920
1-JGHX-20W	342.0	260	660	272	181	1.60	453	404.9	0.00	0	21.9	320.2	214.6	5.7	0.0	747.6	0.0000	0.0497	1.346
1-JGHX-20X	350.0	260	660	272	181	1.60	453	398.8	0.00	2	21.9	315.0	214.4	4.9	0.0	648.4	0.0000	0.0412	1.323
1-JGHX-20Y	358.5	260	660	272	181	1.60	453	393.5	0.00	0	21.8	314.8	221.4	6.1	0.0	648.4	0.0000	0.0427	1.302
1-JGHX-20Z	366.0	260	660	272	181	1.60	453	392.5	0.00	0	24.8	313.4	219.7	5.2	0.0	648.4	0.0000	0.0439	1.481
1-JGHX-20AA	374.0	260	660	323	131	2.47	464	306.3	0.00	6	77.0	622.5	251.0	11.2	1.6	947.0	21.0122	0.0426	2.135
1-JGHX-20AB	383.3	260	660	323	131	2.47	464	304.3	0.00	9	60.9	628.8	233.0	11.1	1.1	947.1	14.8123	0.0421	2.495
1-JGHX-20AC	390.0	260	660	323	131	2.47	464	341.7	0.00	9	82.6	640.3	226.7	13.1	1.9	946.9	29.0460	0.0555	2.570
1-JGHX-21A	398.0	260	660	323	131	2.47	464	388.8	0.00	9	83.3	636.2	227.7	12.9	2.0	946.5	34.5634	0.0622	2.933
1-JGHX-21B	407.3	240	760	302	151	2.00	453	387.2	0.00	2	37.9	481.3	239.6	4.4	0.1	746.5	2.7655	0.0268	1.656
1-JGHX-21C	414.0	240	760	302	151	2.00	453	389.5	0.00	1	33.5	481.1	245.1	3.4	0.2	748.4	5.1052	0.0207	1.471
1-JGHX-21D	422.0	240	760	302	151	2.00	453	377.8	0.00	0	32.7	482.1	244.3	4.2	0.2	746.6	3.8946	0.0248	1.389
1-JGHX-21E	430.0	240	760	302	151	2.00	453	373.4	0.00	1	34.5	480.7	243.3	4.3	0.5	746.2	9.7600	0.0254	1.453
1-JGHX-21F	438.0	260	660	323	131	2.47	464	342.8	0.00	2	67.5	606.5	217.0	15.6	1.2	946.8	18.1610	0.0661	2.070
1-JGHX-21G	470.0	260	660	323	131	2.47	464	292.8	0.00	1	62.1	320.2	564.7	14.7	1.2	946.9	16.5161	0.0533	1.620
1-JGHX-21H	502.2	260	660	323	131	2.47	464	294.0	0.00	1	60.9	325.6	564.0	12.8	0.7	947.6	9.1034	0.0468	1.542
1-JGHX-21I	510.0	269	948	227	76	2.99	303	232.4	0.00	2	67.3	661.6	241.5	0.6	1.4	946.3	14.6054	0.0019	1.405
1-JGHX-21J	510.0	269	948	227	76	2.99	303	226.8	0.00	3	79.0	662.7	201.0	15.7	2.1	945.6	21.9018	0.0442	1.612
1-JGHX-21K	526.5	269	948	227	76	2.99	303	226.6	0.00	4	72.8	605.6	181.5	15.7	2.5	940.7	25.6685	0.0444	1.497
1-JGHX-21L	534.0	269	948	227	76	2.99	303	227.3	0.00	4	77.5	683.2	182.2	14.3	3.0	942.5	30.9396	0.0406	1.599
1-JGHX-21M	542.0	269	948	227	76	2.99	303	227.3	0.00	4	76.3	609.0	178.1	15.6	2.6	944.0	26.7106	0.0441	1.571
1-JGHX-21N	560.0	260	946	227	76	2.99	303	228.8	0.00	4	86.3	675.0	176.8	15.0	2.8	940.4	29.0230	0.0430	1.839
1-JGHX-21O	564.0	260	949	227	76	2.99	303	226.4	0.00	2	67.3	733.4	159.0	0.5	2.6	945.6	26.4850	0.0015	1.369
1-JGHX-21P	550.0	260	948	668	335	1.99	1003	862.4	0.00	11	39.8	620.2	295.7	5.1	0.0	946.0	37.0143	0.0545	3.095
1-JGHX-21Q	566.0	260	948	668	335	1.99	1003	910.7	0.00	2	26.1	617.6	312.5	4.4	0.6	946.9	24.1527	0.0501	2.122
1-JGHX-21R	574.0	260	948	668	335	1.99	1003	909.5	0.00	2	28.4	616.0	311.5	4.4	0.7	945.7	27.1752	0.0497	2.309
1-JGHX-21S	582.0	260	952	169	84	2.01	253	176.1	1.33	4	89.3	581.5	280.3	30.4	2.0	946.8	16.0697	0.0665	0.999
1-JGHX-21T	590.0	260	952	169	84	2.01	253	217.0	3.21	18	149.4	546.3	227.8	39.3	2.0	946.9	19.9029	0.1058	0.201
1-JGHX-21U	598.0	260	951	169	84	2.01	253	217.0	3.21	22	170.6	528.3	242.9	21.0	1.7	948.1	17.0267	0.0664	0.314
1-JGHX-21V	608.0	260	952	169	84	2.01	253	219.1	3.50	24	174.0	524.1	248.1	16.4	1.9	947.9	18.8911	0.0445	0.250
1-JGHX-21W	638.0	260	952	169	84	2.01	253	232.7	3.89	24	172.0	522.5	264.4	13.4	1.6	947.7	17.0463	0.0388	0.332
1-JGHX-21X	670.0	261	952	169	84	2.01	253	232.3	3.89	26	188.2	523.7	257.9	13.6	2.4	946.7	26.6986	0.0392	0.202
1-JGHX																			

Table 16. Summary of Designed Set #2. Pressure = 950 psia, H₂/CO = 2:1.

Run	Temperature °C	Gas Feed SCCM	MeOH Feed g/hr	MeOH Prod g/hr
1	260	1000	0	2.216
2	220	250	0	.564
3	260	250	3.5	.295
4	220	1000	3.5	.112
CP	240	500	1.7	.586

FIGURE 2

INITIAL METHANOL PRODUCTIVITY

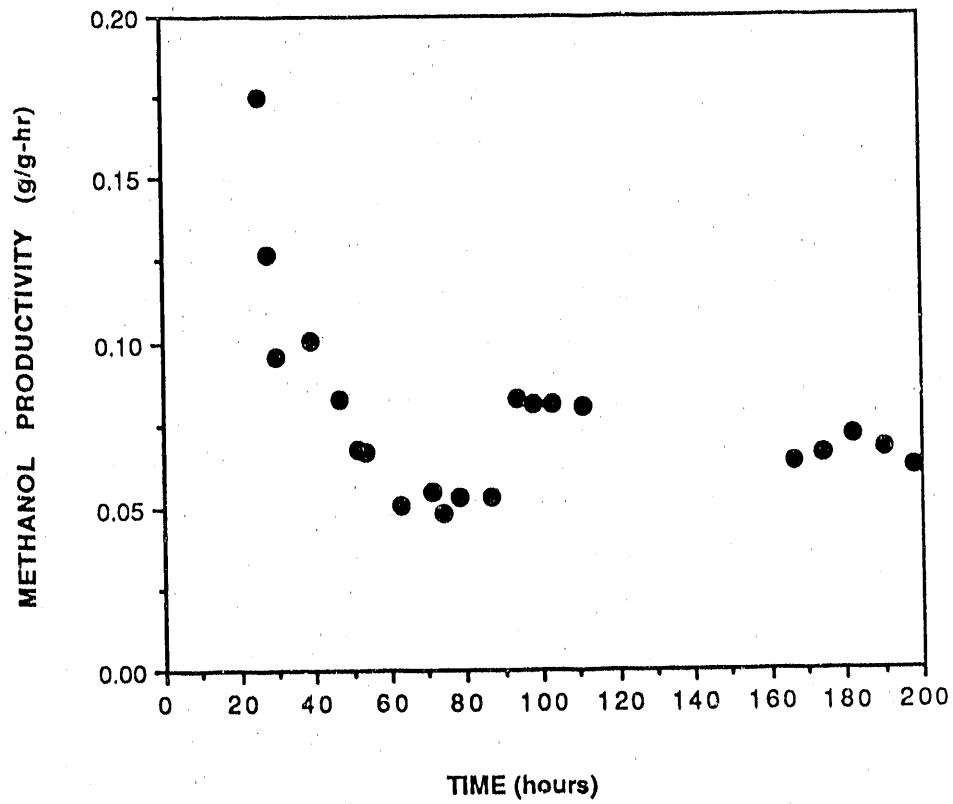
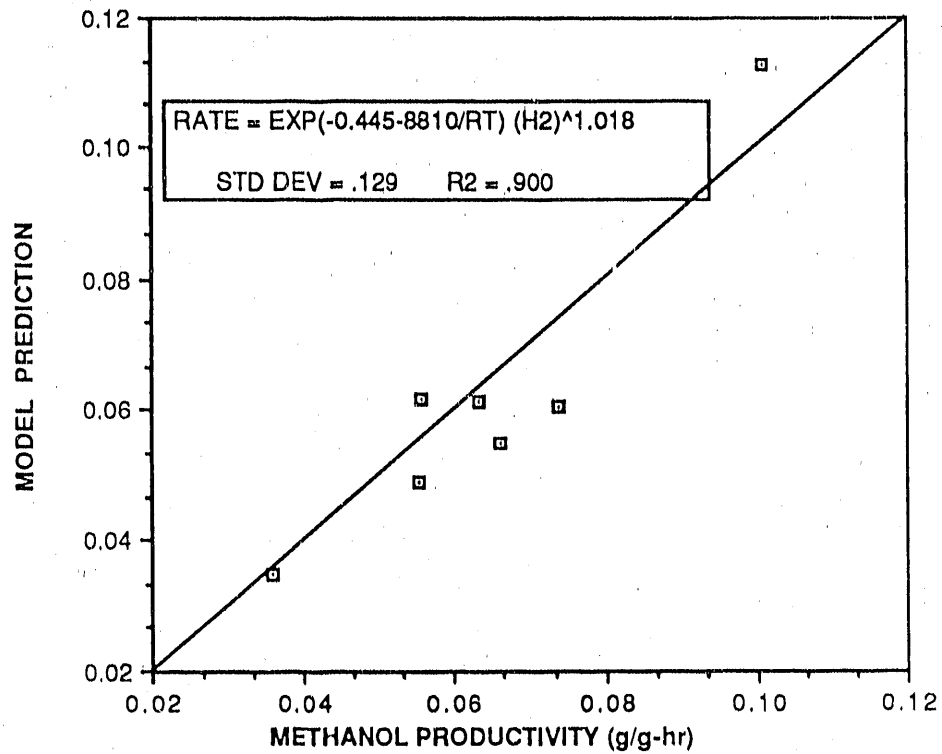


FIGURE 3
COMPARISON OF MODEL PREDICTION
WITH RESULTS FROM DESIGN SET #1



CONDITIONS:

RUN	TEMPERATURE °C	PRESSURE PSIA	H2 FEED SCCM	CO FEED SCCM	H2:CO
1	220	550	323	131	2.5
2	220	950	272	181	1.5
3	260	550	272	181	2.5
4	260	950	323	131	2.5
CP	240	750	300	150	2.0

(GHSV=1000 Sl/hr-Kg)

FIGURE 4
METHANOL PRODUCTIVITY FROM CENTER-POINT RUNS
SHOWING DEACTIVATION RATE OF CATALYST

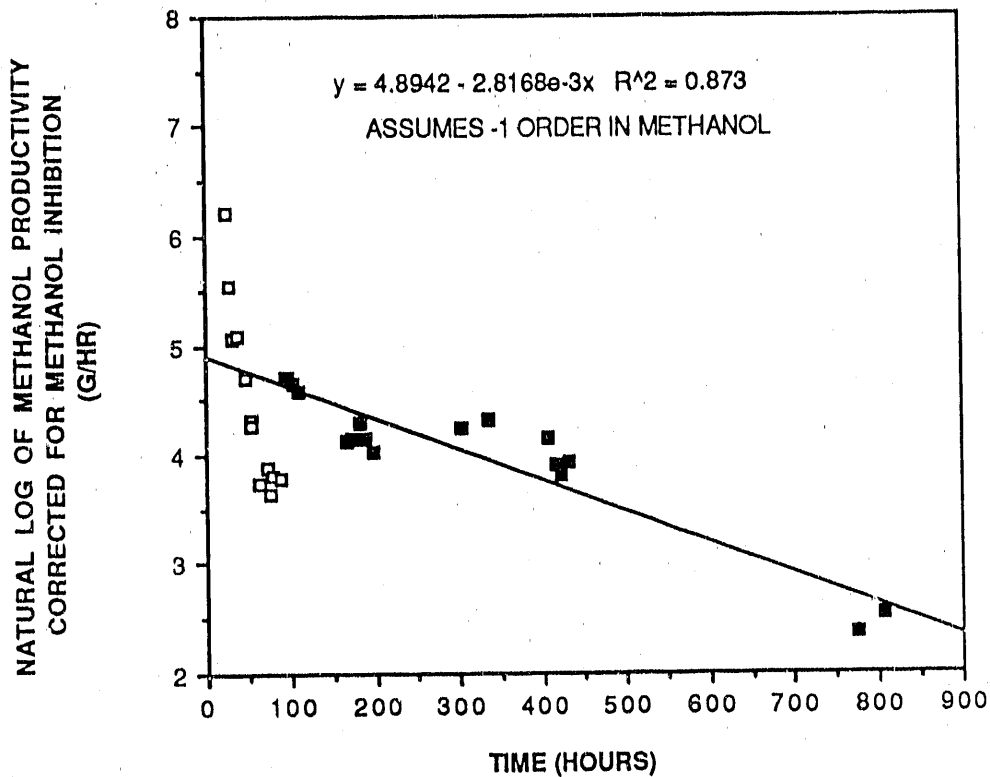
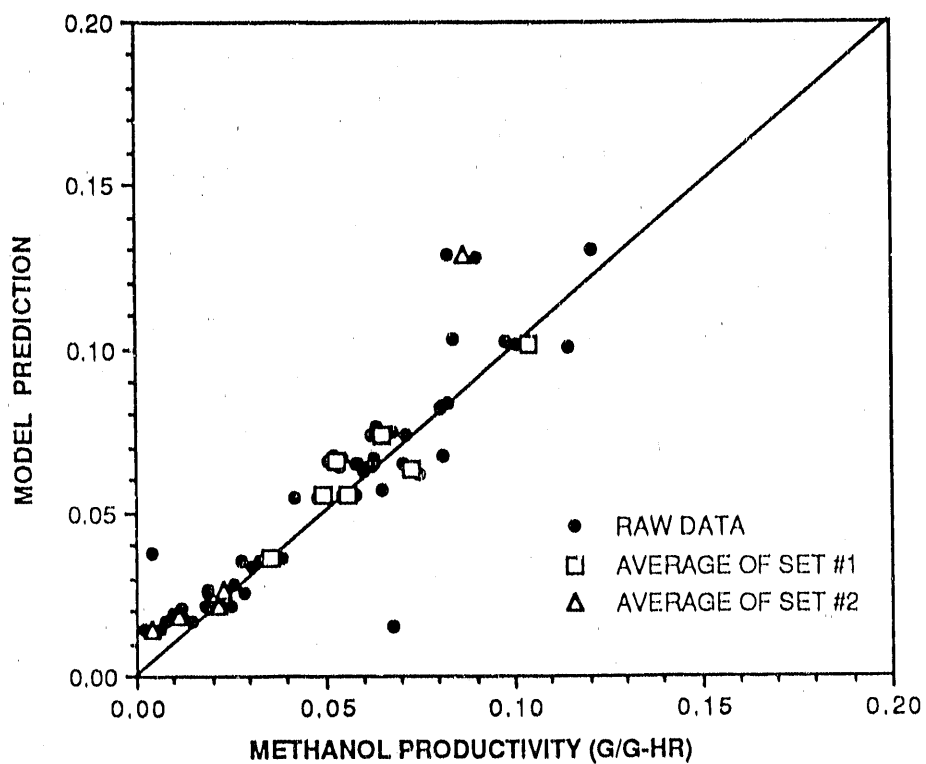


FIGURE 5

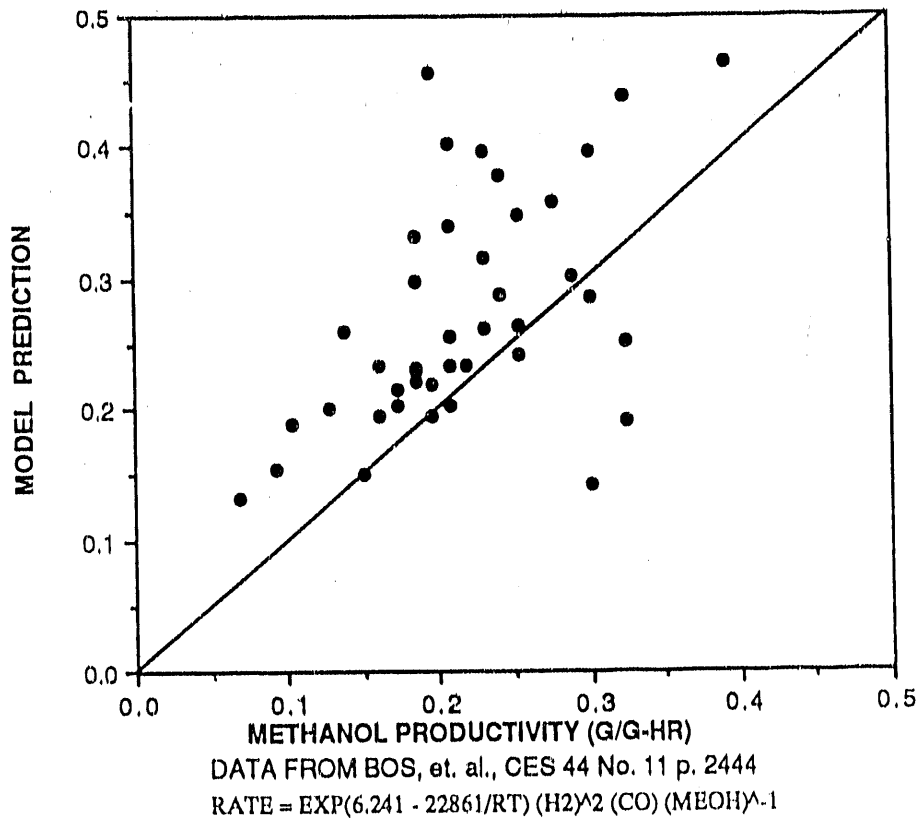
COMPARISON OF METHANOL PRODUCTIVITY WITH MODEL PREDICTION



$$\text{RATE} = \text{EXP}(6.241 - 22861/\text{RT} - 0.002817t) (\text{H}_2)^2 (\text{CO}) (\text{MEOH})^{-1}$$

FIGURE 6

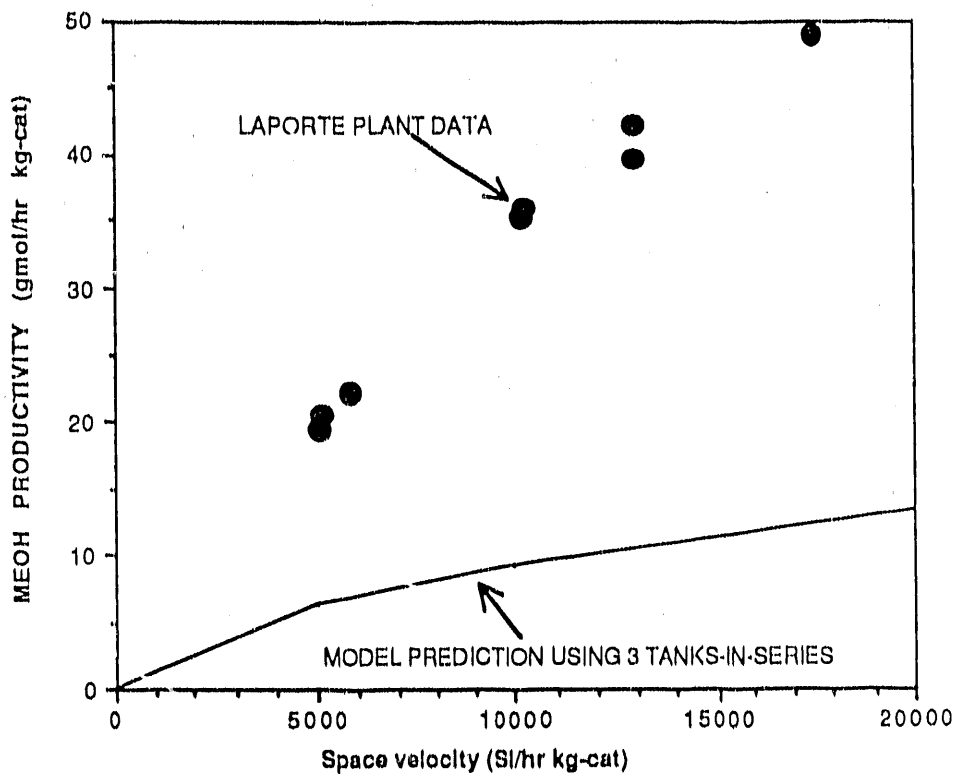
COMPARISON OF MODEL PREDICTION WITH PUBLISHED DATA



The reaction was carried out in a Berty reactor (gas-phase)
Pressure = 400 - 1000 psig
Temperature = 230 - 280 °C
H₂:CO = 3.5:1 - 24:1
GHSV = 6000 SL/KG-HR
Catalyst = BASF S3-85 Cu/ZnO/α-Al₂O₃

FIGURE 7

COMPARISON OF MODEL PREDICTION WITH
PRODUCTIVITY FROM LAPORTE LPMEOH PDU REACTOR



CONTINUOUS SLURRY REACTOR (2' ID x 20' TALL)

750 PSIG

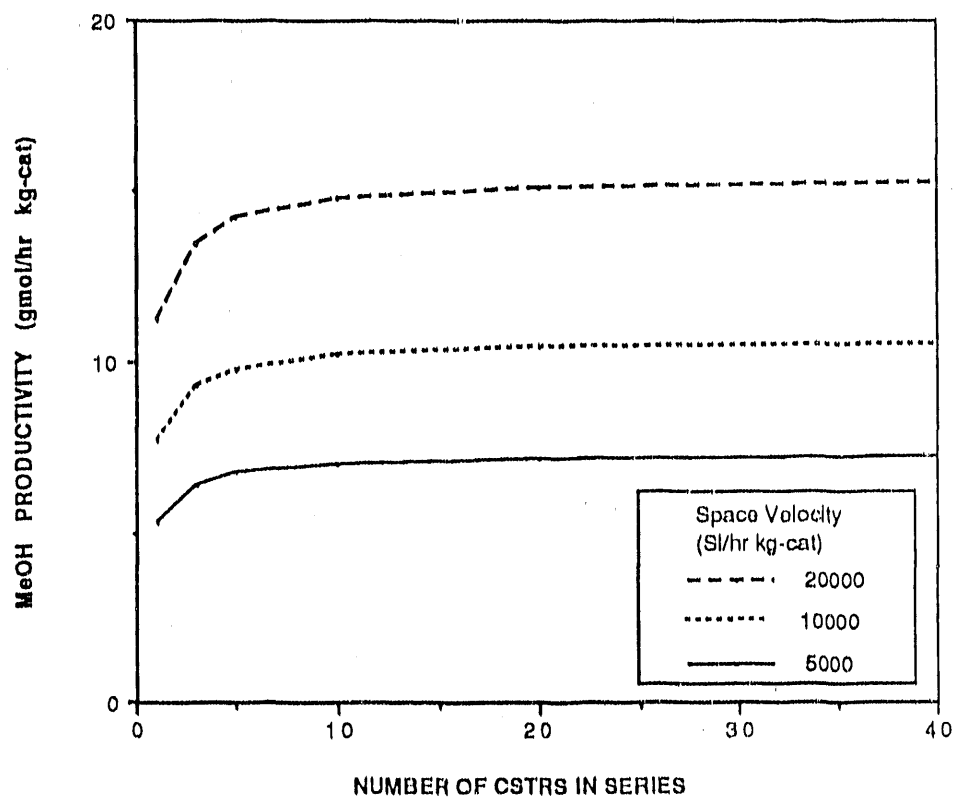
250°C

35% H₂; 51% CO; 13% CO₂; 1%N₂

MeOH PRODUCTIVITY = 5 - 10 TPD

FIGURE 8

EFFECT OF FLOW PATTERN ON MEOH PRODUCTIVITY



NOTE: PRODUCTIVITY CORRESPONDS TO 2 - 5 PERCENT CONVERSION

FIGURE 9

CARBON BALANCE OVER REACTOR

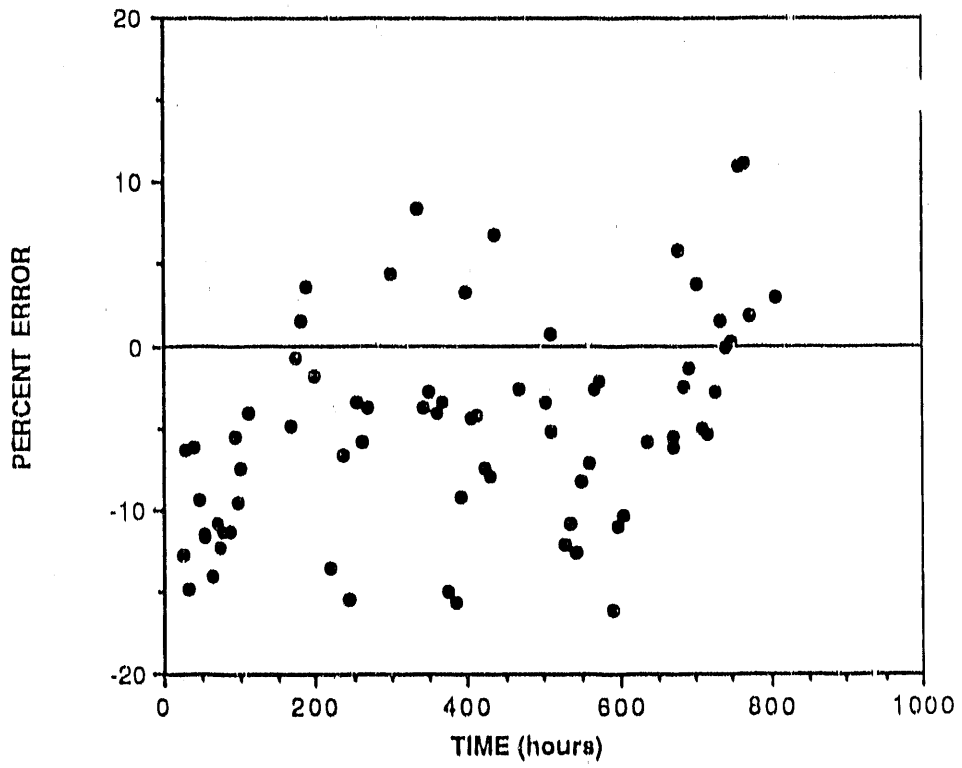


FIGURE 10

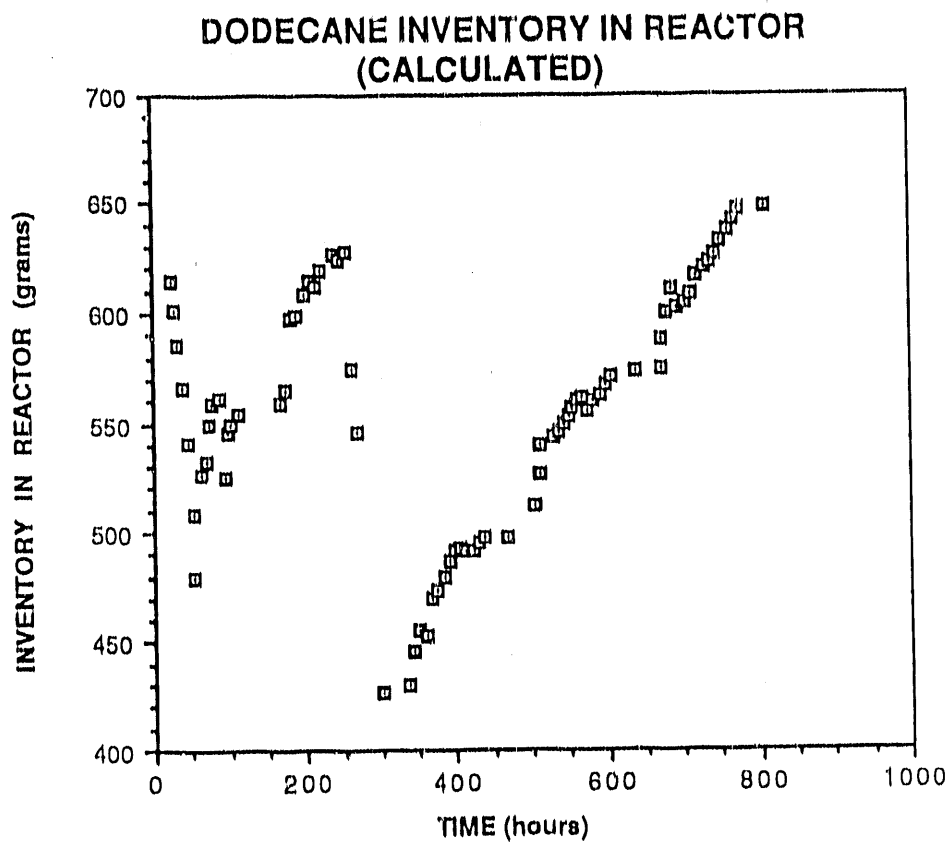
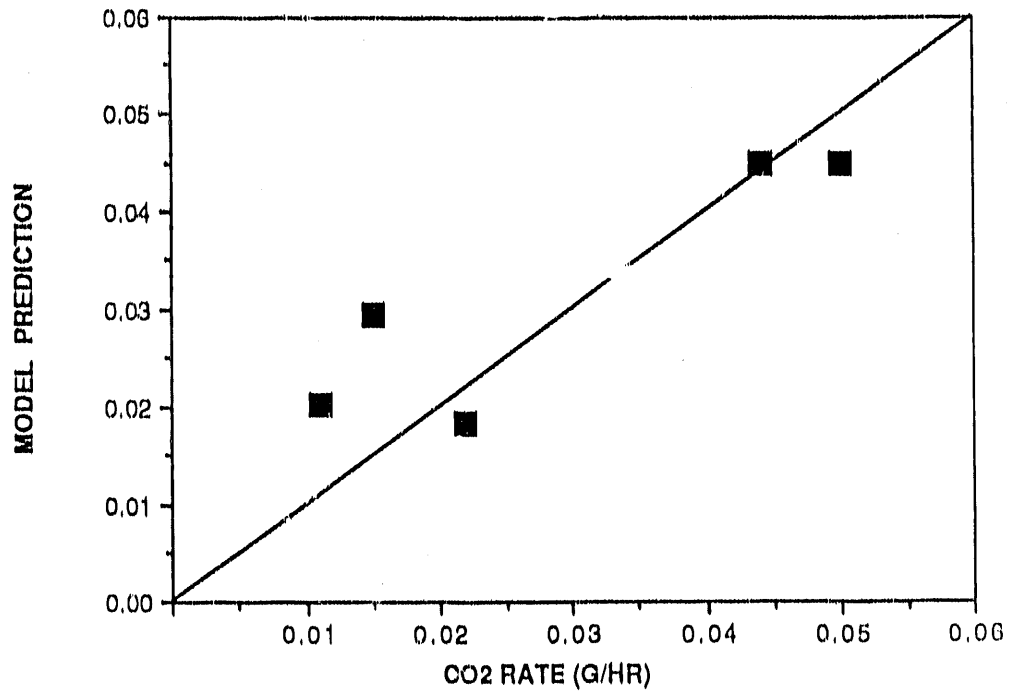


FIGURE 11

PRODUCTION RATE OF CO2 IN DESIGN SET #2

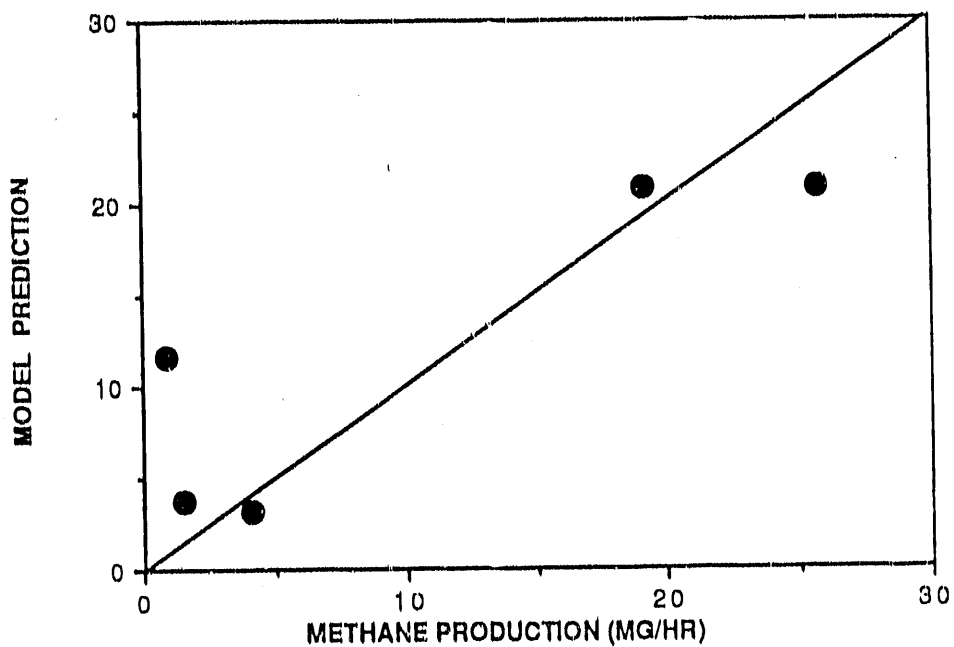


$$\text{RATE (mg/hr)} = e^{(12.323-16344/RT)}$$

INDEPENDENT OF METHANOL PARTIAL PRESSURE

FIGURE 12

METHANE PRODUCTION FROM DESIGN SET #2



$$\text{RATE (mg/hr)} = e^{(38.867 - 32228/RT)}$$

INDEPENDENT OF METHANOL PARTIAL PRESSURE

B. Task 3 Summary

The slurry reaction system was successfully started up using a standard Cu/Zn/Al methanol catalyst (CCI #6341) to test the performance of the system and demonstrate our ability to obtain quality kinetic data. The results of these tests showed: 1) tetraglyme (tetraethylene glycol dimethyl ether) is not a good solvent for the process, 2) using dodecane as a solvent, we were able to obtain quality data which gave us a good material balance, and 3) a kinetic model developed from the dodecane data was able to predict methanol productivity reported by other researchers. We plan to perform a few more tests using different activation techniques before testing the catalyst developed under Task 2 of this effort.

The methanol catalyst was tested for 216 hours in the slurry reactor using tetraglyme as the solvent. At 240°C, with stoichiometric H₂:CO feed, pressure between 750 and 950 psig and GHSV of 1000 SI/kg-hr, the methanol productivity dropped from 0.04 g/g-hr to around 0.003 g/g-hr in 100 hours. Reactivating the catalyst in situ restored about half of the original activity, but again the productivity quickly dropped off to less than 0.005 g/g-hr.

The methanol catalyst was tested for 806 hours in the slurry reactor using dodecane as the solvent. During this test, our dodecane material balance was within a few percent. An elemental carbon balance (excluding dodecane) was typically within ten percent.

Two experimental designed sets were run during this test along with several center-points in order to determine the catalyst's deactivation rate. The first design set was developed to determine the effects of temperature and partial pressure of hydrogen and carbon monoxide. This set indicated that methanol was inhibiting the reaction even though we were operating far from equilibrium, so a second set was run to determine the effect of methanol inhibition. Regression of the data sets produced the following model for the production rate of methanol.

$$\text{RATE (g/g-hr)} = \frac{(\text{H}_2)^2 (\text{CO})}{(\text{MeOH})} e^{(6.241 - 22861/\text{RT} - 0.002817t)}$$

The concentrations are the partial pressures (psi), the temperature is in K, and the time is in hours. This model provided a good fit of the experimental data. The model was also able to predict the results of literature and plant data with reasonable accuracy. The catalyst deactivated at a rate of 0.28%/hour in this test, this is over an order of magnitude better than the test using tetraglyme as the solvent.

- END -

DATE FILMED

11 / 1 / 90

